Study of sequential abiotic and biotic degradation of styrene butadiene rubber

Laurie Calarnou, Mounir Traïkia, Martin Leremboure, Sandrine Therias, Jean-Luc Gardette, Pierre-Olivier Bussière, Lucie Malosse, Séverin Dronet, Pascale Besse-Hoggan, Boris Eyheraguibel

Study of sequential abiotic and biotic degradation of styrene butadiene rubber

Laurie Calarnou[1], Mounir Traïkia[1,2], Martin Leremboure[1], Sandrine Therias [1], Jean-Luc Gardette [1], Pierre-Olivier Bussière [1], Lucie Malosse[3], Séverin Dronet[3], Pascale Besse-Hoggan[1], Boris Eyheraguibel[1]

[1] Université Clermont Auvergne, Clermont Auvergne INP, CNRS, Institut de Chimie (ICCF), F-63000 Clermont– Ferrand, France.

[2] Université Clermont Auvergne, Plateforme d'Exploration du Métabolisme, MetaboHUB Clermont, Clermont-Ferrand, France

[3]Manufacture Française des Pneumatiques MICHELIN, Centre de Technologies Ladoux, 63040 Clermont-Ferrand, France.

Keywords

Photo-ageing; Thermo-ageing; Biodegradation, *Rhodococcus ruber* ATCC29672; *Gordonia polyisoprenivorans* VH2

Abstract

Styrene butadiene rubber is one of the main constituents of tire tread. During tire life, the tread material undergoes different stresses that impact its structure and chemical composition. Wear particles are then released into the environment as weathered material. To understand their fate, it is important to start with a better characterization of abiotic and biotic degradation of the elastomer material. A multi-disciplinary approach was implemented to study the photo- and thermo- degradation of non-vulcanized SBR films containing 15 w% styrene as well as their potential biodegradation by *Rhodoccocus ruber* and *Gordonia polyisoprenivorans* bacterial strains. Each ageing process leads to crosslinking reactions, much surface oxidation of the films and the production of hundreds of short

chain compounds. These degradation products present a high level of unsaturation and oxidation and can be released into water to become potential substrates for microorganisms. Both strains were able to degrade from 0.2 to 1.2 % (% ThOD) of the aged SBR film after 30-day incubation while no biodegradation was observed on the pristine material. A 25-75 % decrease in the signal intensity of water extractable compounds was observed, suggesting that biomass production was linked to the consumption of low-molecular-weight degradation products. These results evidence the positive impact of abiotic degradation on the biodegradation process of styrene butadiene rubber.

1. Introduction

Styrene butadiene rubber (SBR) is the main elastomer in the formulation of car tire treads and one of their main components (30-70 wt%) (Babbit, 2010; Baumann and Ismeier, 1998). During the use phase on the road, the tire undergoes various physico-chemical stresses such as mechanical shear stress that leads to the degradation and release of SBR into the environment as tire and road wear particles (TRWP). Once generated, these particles are transported into various environmental compartments (air, soil, runoff, estuaries, sediments) (Baensch-Baltruschat et al., 2021; Goßmann et al., 2021; Klöckner et al., 2021, 2020; Leads and Weinstein, 2019; Panko et al., 2013; Parker-Jurd et al., 2021; Rauert et al., 2022; Unice et al., 2012), where further SBR degradation processes can occur, such as photo and thermooxidation and/or microbial degradation (Wagner et al., 2022). Large masses of TRWP released into the environment (0.2 to 5.5 kg/inhabitant/year) raise concerns about their potential impact on the ecosystems and questions about their persistence and fate (Baensch-Baltruschat et al., 2020). A thorough characterization of the complex chemical composition of TRWP is thus necessary to better understand the transformation of these particles. Such a task is challenging as the abiotic and biotic transformation of the elastomers and formulating agents in tire tread composition must be considered. While several studies recently identified the transformation products (*e.g.* 6PPD quinone, benzothiazole) of some tire curing and protective agents resulting from abiotic ageing (Calarnou et al., 2023; Fohet et al., 2023; Hu et al., 2022; Seiwert et al., 2022; Thomas et al., 2022; Unice et al., 2015), literature concerning the fate of elastomers is quite limited and often based

on the study of model materials. The effect of light on the ageing of vulcanized rubber was first shown in 1926 (Jecusco, 1926). Much research work subsequently studied the effects of UV, temperature or ozone on non-vulcanized 1,4-cis-isoprene rubber (IR), butadiene rubber (BR) and SBR (Adam et al., 1989a; Chandra, 1983; Lacoste et al., 1994) and vulcanized SBR and natural rubber (NR) (Osswald et al., 2019; Thomas et al., 2022) to predict their impacts on rubber/tire properties and performance. The mechanisms of photo and thermo-degradation of SBR were proposed for the first time in 1989 by Adam et al. (1989a). In the presence of oxygen, UV radiation and temperature induce significant modifications in the molecular network of SBR through cross-linking and cleavage reactions, resulting in the formation of oxidized degradation products with a reduced molecular weight (Chandra, 1983). The photo and thermooxidized SBR present various new functional groups including hydroperoxides, α,β-unsaturated ketones and saturated ketones, acids, alcohols and epoxides (Adam et al., 1989a). In ageing studies, the occurrence of such degradation products in polymers is conventionally measured by FTIR spectroscopy (Wilhelm and Gardette, 1994) and combined with physico-chemical characterization to evaluate the loss of material properties. Nevertheless, the formation rate of degradation products, their characterization and their leaching potential into the environment remain understudied. Recently, Thomas et al. (2022) proposed a list of possible transformation products of elastomers resulting from thermal or photo-ageing of tire cryogrinds. Oxidation products such as carboxylic acids, ketones and epoxides were detected in THF extracts by GC/MS. These components as well as the residual solid matrix of the elastomer (crosslinked and non-crosslinked) must be considered as potential carbon sources for microorganisms.

The current literature on synthetic elastomer biodegradation is mainly focused on biotechnological approaches for the purpose of rubber waste recycling. In that context, several studies used either actual tire tread materials (Tsuchii et al., 1996; Tsuchii and Tokiwa, 1999), ground tire rubber (Cui et al., 2016; Li et al., 2012, 2013) or model vulcanized rubber (Aboelkheir et al., 2019; Hu et al., 2016) where the elastomer and all the additives can potentially serve as substrates for microorganisms. Aboelkheir et al. (2019) showed surface modifications and suggested carbon and sulfur bond cleavages of vulcanized SBR in the presence of *Bacillus subtilis*, *Pseudomonas aeruginosa* and

Streptomyces sp. Other strains, including *Gordonia* spp, *Sphingomonas*, *Acidithiobacillus* and *Acinetobacter* spp., were also studied for their abilities to devulcanize SBR by the cleavage of the sulfur bonds (Cui et al., 2016; Hu et al., 2016; Li et al., 2012, 2013). Conversely, studies on pure SBR or BR are very scarce (Nielsen et al., 2023; Williams, 1982). In 1984, Tsuchii et al. isolated a *Moraxella* strain from soil capable of degrading more than 40 % of 1,4-BR with a molecular weight (Mn) under 2,500 within 5 days.

Besides SBR and BR, many studies focused instead on the biodegradation of natural or synthetic IR, another elastomer entering tire formulation and other manufactured products (*e.g.* gloves, hoses, gaskets, conveyor belts). IR biodegradation was demonstrated by several pure microbial strains (Andler et al., 2022; Berekaa, 2006; Berekaa et al., 2000; Borel et al., 1982; Cheng et al., 2023; Ibrahim and El-ameen, 2013; Linos et al., 2000; Roy et al., 2006; Tsuchii et al., 1979) or by a consortium (Nguyen et al., 2020). Its metabolic pathways were particularly investigated for the bacteria *Gordonia polyisoprenivorans* VH2 (Hiessl et al., 2012), *Streptomyces* sp. K30 (Rose et al., 2005) and *Xanthomonas* sp. 35Y (Birke et al., 2017; Sharma et al., 2018). It was shown that the oligo-isoprenoids formed, resulting from the cleavage of the double bonds of the isoprene units, can be bio-assimilated by microorganisms (Bode et al., 2000; Hiessl et al., 2012).

In the environment, abiotic and biotic degradation processes occur simultaneously or consecutively. The impact of abiotic transformations of rubber on biodegradation has never been considered to our knowledge. In 1980, Cadle and Williams studied the environmental degradation of tire wear particles (TWP) in roadside soil and suggested that the elastomer degradation was mainly due to atmospheric oxidation rather than microbial attack (Cadle and Williams, 1980). Biodegradation of SBR can occur in environmentally aged roadway particles (see our recent work Calarnou et al., 2023). Herein, *R. ruber* ATCC 29672 was found to degrade 12 % of the SBR extractable fraction from TRWP within 14 days. Photo and thermooxidation of polymers (polyethylene, polypropylene) have already been reported to produce short oxidized chains that are subsequently used by microorganisms as carbon substrates (Albertsson and Karlsson, 1990; Bonhomme et al., 2003; Corti et al., 2010; Eyheraguibel et al., 2017; Fontanella et al., 2013; Koutny et al., 2006; Rodrigo et al., 2021). From an environmental standpoint, biotic and abiotic degradations control the fate of chemicals. Therefore, assessing

biodegradation of such polymers, generally considered difficult to (bio)degrade, should integrate their prior abiotic chemical transformations and the variety of degradation carbon sources they can generate.

The present study continues our work on the biodegradation of roadway particles containing TRWP (Calarnou et al., 2023) that characterized the various potential carbon sources present (elastomers, plasticizers, curing agents, antioxidants and their degradation products) describing their biodegradation. The complexity observed in TRWP hindered understanding (bio)degradation of each compound, especially of the elastomer phase. This study therefore aimed to investigate the impact of photo and thermooxidation processes on the biotic degradation of a pure uncrosslinked SBR sample, as a simpler system. Accelerated ageing studies were conducted to characterize the chemical modifications of the elastomer by these abiotic processes and quantify the degradation products formed by a multi analytical approach. The impact of abiotic degradation on biodegradation was assessed by monitoring the growth of two bacterial strains, belonging to two ubiquitous genera, *Rhodococcus ruber* ATCC 29672 and *Gordonia polyisoprenivorans* VH2 in the presence of pristine and variously oxidized SBR samples. The various sources of carbon (leachable and extractable compounds and SBR matrix) that could be potential substrates for microorganisms were monitored during biodegradation.

2. Materials and methods

2.1. Chemicals and reagents

All the solvents used for extraction were HPLC analytical grade. Acetone and tetrahydrofuran (THF) stabilized with 2,6-di-tert-butyl-4-methylphenol (THF stabilized with BHT, Analytical grade, q.s. 1 g/L) were obtained from Sigma Aldrich. Deuterated water supplemented with 0.2 mM $TSPd_4$ (sodium tetra deuterated trimethylsilyl propionate) and acetone-d_6 supplemented with 0.03 v/v % TMS (tetramethylsilane) were purchased respectively from Eurisotop and InnovaChem.

2.2. Sample preparation

Two elastomers, provided by Michelin, were tested: a non-vulcanized styrene-butadiene rubber (SBR) containing 15 w% styrene, 20 w% 1,2-butadiene, 65 w% 1,4-butadiene (Mn ~210 $kg.mol^{-1}$, Mw ~413 $kg.mol^{-1}$) and a synthetic *cis*-1,4-polyisoprene (IR) (Mn ~400 $kg.mol^{-1}$). To remove antioxidants, SBR and IR, solubilized in toluene (solution at 100 $mg.mL^{-1}$ and 50 $mg.mL^{-1}$ for SBR and IR, respectively), were precipitated in 2 volumes of ethanol. The washing step was repeated on the coagulum twice. The elastomers were then vacuum-dried on an aluminum tray in an oven at 45 °C under nitrogen flux for about 40 h, down to a constant weight. The elastomers were then stored in sealed septum vials under inert atmosphere (nitrogen) in the dark at -25 °C.

2.3. Abiotic degradation

50 µm thick films were prepared by compression molding between silicone-coated polyester clothes (SRF121, HiFi Industrial Film), first in contact for 30 s at 110 °C and then pressed at 50 bars for 1 min at 110 °C. As the films obtained were not self-standing, they were aged directly on silicone-coated polyester clothes or placed onto CaF_2 pellets (Crystran) to facilitate further experiments.

Photoageing experiments were conducted using a Suntest CPS/XLS Atlas device, equipped with an ATLAS (NXE1700) xenon lamp set at 500 $W.m^{-2}$ in the UV-visible domain (300–800 nm) (Potaufeux

et al., 2022). Infrared irradiation and UV photons below 300 nm were cut off using an Atlas ‘‘daylight filter’’. A cryostat was used to maintain the black standard temperature (BST) at 60 °C, corresponding to *ca.* 37 °C in the irradiation chamber.

Thermooxidative ageing was carried out in a forced air venting oven (Memmert UF30) at 80 °C.

2.4. Biodegradation

Preparation of the inoculum. Two bacterial strains were selected for the biodegradation experiments: *Rhodococcus ruber* ATCC 29672 and *Gordonia polyisoprenivorans* VH2 (DSMZ 44266). They were cultivated at 27 °C for 24 h in shake flasks containing 10 mL of tryptic soy (TS) broth. Aliquots of both cultures (2 mL) were centrifuged at 9,700×*g* during 5 min and resuspended in NaCl solution (8% w/v). Pellets were washed two times more and finally resuspended in 2 mL of mineral salt medium (MSM). MSM was prepared as follow: $Na_2HPO_4.12H_2O$, 3.8 $g.L^{-1}$; KH_2PO_4, 1.8 $g.L^{-1}$, $MgSO_4,7H_2O$, 20 $mg.L^{-1}$; $Fe(NH_4)_2(SO_4)_2.6H_2O$, 30 $mg.L^{-1}$; $CaCl_2.2H_2O$, 10 $mg.L^{-1}$; NaCl, 0.5 $g.L^{-1}$, NH_4Cl, 0.3 $g.L^{-1}$; $MnSO_4.H_2O$, 18.5 $mg.L^{-1}$, H_3BO_3, 20 $mg.L^{-1}$; $ZnSO_4.7H_2O$, 2.5 $mg.L^{-1}$; $Na_2MoO_4.2H_2O$, 2.5 $mg.L^{-1}$; $CoSO_4$ 8 $\mu g.L^{-1}$ and $CuSO_4.5H_2O$ 8 $\mu g.L^{-1}$.

Biodegradation experiments. Biodegradation assays were performed in 50 mL sterile glass flasks. Strains were inoculated at 10^6 $cell.mL^{-1}$ from the previously prepared cell suspension in 10 mL of MSM containing or not (biotic control) 100±5 mg of SBR films as the sole carbon source. The films were previously sterilized, directly in the culture flasks, by soaking with 1 mL of 70 % ethanol until total evaporation of the ethanol. Bacteria were cultivated on four SBR materials: pristine SBR (“SBR”), photooxidized SBR (“SBR-photo-30h”) and two thermooxidized SBR (“SBR-thermo-168h” and “SBR-thermo-330h”). In parallel, bacteria were also cultivated on pristine IR in the same conditions for comparison. The condition *Gordonia*/IR was used as a positive control. Incubations of SBR and IR materials without bacteria were also performed as abiotic controls (AB). The experiments were carried out in duplicate for each condition, for 30 days at 27° C and 130 rpm in an Innova 44 incubator (Eppendorf).

Bacterial growth. Biologic oxygen demand (BOD) of each culture was monitored using respirometric BOD Oxitop (WTW). Flasks were hermetically closed by Oxitop heads, which recorded BOD values every 120 min. BOD measurements were converted to percentage of biodegradation (% ThOD) by calculating the ratio of the oxygen consumption to the theoretical amount of consumed oxygen for complete degradation of the elastomer (ThOD) (Equation 1 and. 2, SI) according to the standard method ISO 14851 (ISO 14851:2019). At the end of the experiment, the growth of bacteria was determined by measuring the total ATP of culture using ATP Biomass Kit HS (Biothema).

Extracellular protein content (Bradford assay). At the end of the biodegradation experiment, a supernatant aliquot (500 µL) was centrifuged at 9,700 × *g* during 5 min. to remove cells. In a transparent 96-well plate, 150 µL of Bradford solution (ThermoFischer) were added to 150 µL of the cell-free supernatant of each experiment. After 5 min of incubation, the plate was read at 595 nm in a Safire II® microplate reader (Tecan). Extracellular protein content was determined for each sample in duplicate according to the bovine serum albumin (BSA) calibration.

2.5. Sample characterizations.

From the pristine material, the abiotic and biotic degradation generate two distinct experimental series of samples comprising the residual film and the leachable and extractable short oxidized chains. For abiotic degradation samples, the films were characterized by Fourier Transform Infrared spectroscopy (FTIR), Gel fraction and the soluble fraction by size exclusion chromatography (SEC), upon the ageing experiments. The short oxidized chains were extracted from a 20 mg SBR film in 2 mL of sterile distilled water or acetone to distinguish the readily extractable (water-soluble) fraction from less soluble compounds (acetone-soluble). Extractions were performed in duplicate in sterile glass vials, on a horizontal shaker at 200 rpm and 25°C in an incubator (Bioconcept, Firlabo). The extracts were collected after 7 days of incubation. The water- and organo-soluble short oxidized chains were characterized by ^{1}H nuclear magnetic resonance spectroscopy (NMR), Liquid chromatography coupled with high resolution mass spectroscopy (HRMS) and Total organic carbon (TOC) analysis.

For biotic degradation samples, gel fraction analysis was performed on residual films. The water-soluble short oxidized chains were recovered from the supernatants of culture medium by centrifugation at 9,700×*g* for 5 min to remove cells. The SBR films (100 mg) were recovered from each culture and freeze-dried overnight. A 20 mg aliquot was extracted in 2 mL acetone for 7 days. The water- and acetone-soluble short oxidized chains were characterized by ^{1}H NMR and LC/HRMS.

2.5.1. Infrared analyses

Throughout the photo- or thermooxidative aging process, the kinetic characterization of chemical transformation was carried out by infrared analyzes on a single SBR film Infrared spectra of SBR films coated on CaF2 were recorded in transmission mode with a Nicolet 6700 FTIR spectrometer, working with OMNIC software. Spectra were obtained using 32 scans and a 4 cm-1 resolution. FTIR spectra obtained by attenuated total reflection mode (ATR) were recorded using a Nicolet 380 spectrophotometer equipped with a diamond crystal (refractive index = 2.5). Spectra were recorded with 64 scans at a resolution of 4 cm^{-1}.

2.5.2. Size Exclusion Chromatography (SEC)

Following ageing experiments, degradation of SBR was also evaluated by characterizing the molecular weight distribution of the soluble fraction using SEC. SBR films aliquots (20 ± 5 mg) were dissolved in THF. The solutions were stirred for 2 h then filtered through 0.45 µm disposable syringe filters (PTFE-45/25). The SEC equipment consisted of a degasser, injector and pump (Waters 2695E), a column heater (Waters, ALLCOLHTRB) and a refractive index (RI) detector (Waters, 2414). The columns were three PolyPore InfinityLab, 7.5 x 300 mm (Agilent, PL1113-6500). The columns were maintained at 35° C. The mobile phase was THF at a flow rate of 1.00 $mL.min^{-1}$. The injected volume was 100 µL. The signals obtained with SEC-RI detector were analyzed with Empower software (Waters) using Polystyrene (PS) calibration standards (PSS Polymer, PSS-pskitr1).

2.5.3. Gel fraction determination

To determine the gel fraction, soaking of SBR films (20 mg) was carried out during 72 h in 2 mL of THF at ambient temperature in the dark. Gel and soluble fractions were separated by vacuum filtration on glass fiber filters (Dutscher). The insoluble SBR (gel) was recovered on the filters and was weighted after vacuum drying (3 days at ambient temperature). Gel fractions (Gf in %) were determined by calculating the ratio of the mass of the insoluble SBR to the initial mass of SBR films according to the equation (1).

(1) Gf (%) = [SBR]gel / [SBR]initial * 100

2.5.4. ^{1}H Nuclear Magnetic Resonance spectrometry

^{1}H NMR was used to analyze the water, acetone and THF soluble short chains of SBR after abiotic and biotic degradation. The supernatants from the solvent extractions and biodegradation experiments (1200 µL) were dried under a nitrogen flux and 2-fold concentrated in 600 µL of the corresponding deuterated solvent (D_2O or acetone-d_6 supplemented with a reference)). The NMR analyses were performed on a *Bruker* 500 MHz Avance III spectrometer and the acquisition method was detailed in Calarnou et al. (2023). Briefly, 8 scans were collected (3.24 s acquisition time, 60.0 s relaxation delay, a spectral window of 20 ppm, FID size of 65536 data points zero-filled to 131072 point).

The total NMR signals were integrated to assess the relative quantity of short oxidized chains in the samples and determine their production or consumption. To compare the samples, the total integration of the NMR signals was calibrated according to the internal deuterated standard - TSP for aqueous extracts and TMS for organic extracts (References value equal to 1). The short oxidized chain quantities were expressed in arbitrary units (a.u).

2.5.5. High resolution mass spectrometry

The supernatants (300 µL) from solvent extractions and biodegradation experiments were dried under a nitrogen flux. Samples were 3-fold concentrated by dissolving them in 100 µL of water / acetonitrile mixture (50:50 v:v) for water extracts, or 100 µL of acetone for acetone extracts. HRMS analyses were performed with an Ultimate 3000 RSLC chromatographic system (ThermoScientific) coupled to an Exactive Orbitrap mass spectrometer (Thermo Fisher Scientific) equipped with an electrospray (ESI) source and the chromatographic separation was detailed in Calarnou et al. (2023). The mass spectrometer was operated in positive ion mode and the detection was performed with full scan from m/z 50 to 750 using a resolution set at 70 000 at m/z 200. HRMS raw data were processed with Xcalibur Software (version 4.1). For each sample, all the m/z values detected in the chromatographic run with a peak intensity strictly greater than 10^4 were considered. The molecular formulae were determined by the software algorithm from the exact masses of the m/z (with a mass tolerance of 3 ppm). Due to the chemical nature of SBR and its potential degradation products, single charged ions and only carbon, hydrogen, oxygen atoms and single sodium adducts were considered in the calculation with the following range of atoms: C (1 –100), H (1–200), O (0 –50), Na (0–1). For each feature, the molecular formula was used to determine the number of carbon, hydrogen and oxygen atoms, and to calculate the ratios of H/C and O/C. The complex molecular composition of the samples was presented using Van Krevelen diagrams which consist in plotting the H/C ratio against the O/C ratio (Kim et al., 2003; Van Krevelen, 1950). All the plots were generated using the open-source software pyC2MC (Sueur et al., 2023). To monitor the biodegradation of low-molecular-weight compounds resulting from the abiotic degradation, only the m/z values also present in the abiotic control sample were considered. In the biotic sample data, these values were distinguished and extracted from those of the biomass using a Python script.

2.5.6. Total organic carbon (TOC)

The supernatants (600 µL) of water and acetone extractions prepared after abiotic degradation were dried under a nitrogen flux. The sample duplicates were pooled in 8 mL of ultrapure water before the measurement. The concentration of the total organic carbon (TOC) was determined using a Shimadzu TOC 5050A analyzer.

3. Results and discussions

3.1. Abiotic degradation

Abiotic photochemical- and thermal-ageing of SBR were assessed first by performing kinetic measurements to characterize the gradual chemical transformations of the elastomer in terms of oxidation, crosslinking, and chain scission.

The FTIR spectrum of a SBR film showed the characteristic bands of styrene (1456, 1495, 1582, 1601 cm^{-1}) and of 1-4 and 1-2 butadiene units with the vibrations of methylene groups in the sequence 1,4-*trans* and 1-2, at 966 cm^{-1} and 912 cm^{-1}, respectively (Fig. S1).

3.1.1. Chemical modifications resulting from photooxidation

The FTIR spectra (transmission mode) of SBR films exposed to long wavelength irradiation (λ>300 nm) with oxygen presented various modifications from photooxidation reactions (Fig. 1a, 1b, 1c).

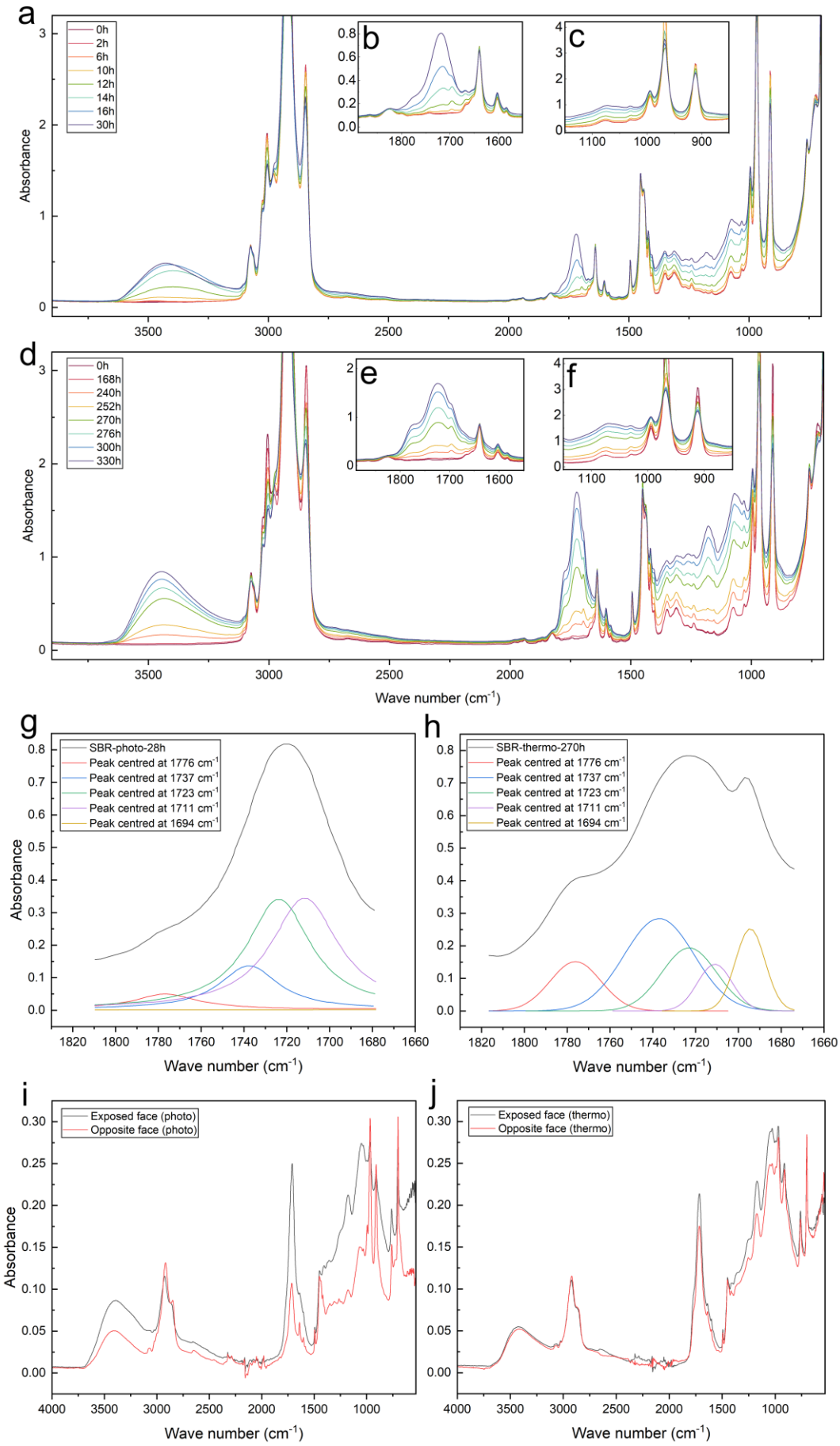
a
0h
2h
6h
10h
12h
14h
16h
30h
Absorbance
b
c
d
0h
168h
240h
252h
270h
276h
300h
330h
e
f
Wave number (cm-1)
g
SBR-photo-28h
Peak centred at 1776 cm-1
Peak centred at 1737 cm-1
Peak centred at 1723 cm-1
Peak centred at 1711 cm-1
Peak centred at 1694 cm-1
h
SBR-thermo-270h
i
Exposed face (photo)
Opposite face (photo)
j
Exposed face (thermo)
Opposite face (thermo)

294

Fig. 1. **a-f)** Transmission FTIR spectra of a SBR film (e = 50 µm) (onto CaF_2) **a-c)** photooxidised at λ> 300 nm, 37° C: a) between 4000-800 cm^{-1}, b) in the carbonyl/carboxyl domain 1900-1550 cm^{-1}, c) in the domain 1150-850 cm^{-1}; **d-f)** during thermooxidation at 80° C: d) between 4000-800 cm^{-1}, e) in the carbonyl domain 1900-1550 cm^{-1}, e) in the domain 1150-850 cm^{-1}. **g-h)** Deconvoluted FTIR spectra after 28 h of photooxidation (g) or 270 h of thermooxidation (h)**. i-j)** ATR-FTIR spectra of the front face (exposed to oxygen) and opposite face for a SBR film onto silicone-coated polyester clothes i) after 30 h of photooxidation j) after 330h of thermooxidation at 80 °C.

Spectral modifications, presented in Fig. 1a to 1c were identified from previous studies performed using chemical derivatization treatments and physical treatments (photolysis, wavelengths effects) (Adam et al., 1990, 1989b, 1989a; Jouan et al., 1989; Wilhelm and Gardette, 1994). In the hydroxyl region (3600-3200 cm^{-1}), a broad absorption band appeared with a maximum around 3460 cm^{-1} corresponding to hydroperoxide and alcohol formation. The carbonyl region in Fig. 1b showed a broadband with a maximum at 1720 cm^{-1} that results from the convolution of two bands (1711 and 1723 cm^{-1}), and a shoulder to this broadband appeared at 1775 cm^{-1}. In the first 10 h of irradiation, an absorption band was observed at 1694 cm^{-1} attributed to αβ–unsaturated ketones, (Adam et al., 1990). The latter are rapidly transformed by addition of radicals to give saturated ketones at 1723 cm^{-1}. Ketones absorb at wavelengths longer than 300 nm and react through Norrish reactions to produce carboxylic acids at 1711 cm^{-1} (Fig. S2). Kinetic monitoring of the absorption band intensities is presented in Fig. 2a, which shows the increase of absorbance of the carbonyl/carboxyl band at 1720 cm^{-1} and the decrease of that of unsaturation at 912 cm^{-1} (the absorbance at 966 cm^{-1} is too high and cannot be used in transmission mode for a 50 µm thick SBR film).

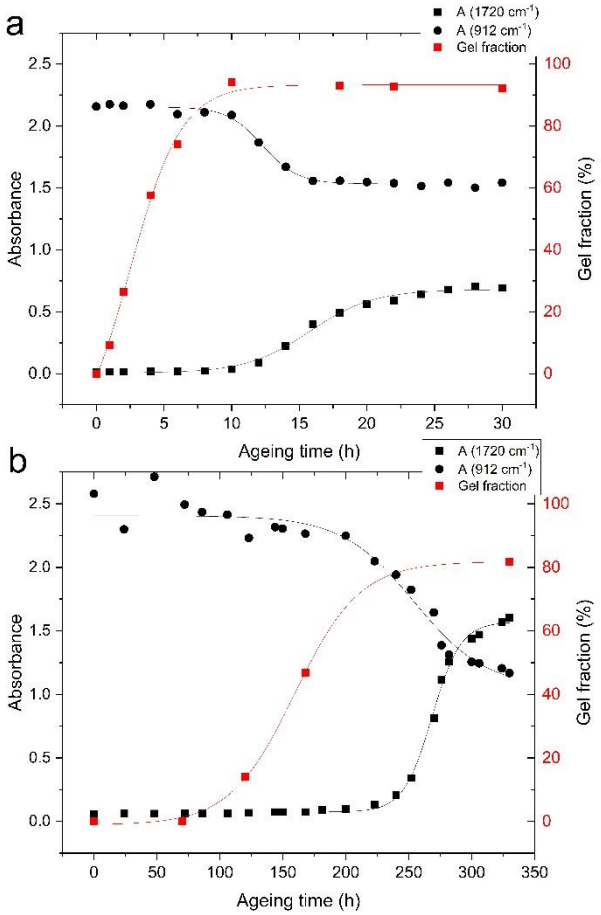

317

318 **Fig. 2**. Variations of absorbance at 1720 cm^{-1} (carbonyl/carboxyl; ■), 912 cm^{-1} (vinyl; ●) and gel
319 fraction level (■) as a function of ageing time for SBR films during (a) photooxidation at λ> 300 nm
320 and (b) thermooxidation at 80° C.

321

322 The shape of the kinetic curves in Fig. 2a indicated that the decrease of the absorbance of the
323 vinyl unsaturation (at 912 cm^{-1}) was inversely proportional to the formation of carbonyls. A period
324 with no detectable oxidation of SBR was observed during the first 10 h of irradiation. Then, the
325 absorbance of the carbonyls (at 1720 cm^{-1}) increased between 10 h and 25 h and reached a plateau
326 with an absorbance around 0.7 (film thickness 50 µm). At the same time, the absorbance of vinyl
327 double bond decreased to 32 % of their initial absorbance up to a plateau corresponding to an
328 absorbance of 1.5. The formation of carbonylated photoproducts and the consumption of double bonds

reached a steady state and photooxidation stopped after about 25 h of irradiation. The styrene absorption bands (1456, 1495, 1582, 1601 cm^{-1}) did not show any significant changes.

3.1.2. Chemical modifications resulting from thermooxidation

The FTIR spectra of SBR films (Fig. 1d, 1e, 1f) submitted to thermal ageing presented modifications like those observed in photooxidation.

However, the relative intensities of the absorption bands in the carbonyl domain were different. The band at 1694 cm^{-1} increased along thermooxidation, and the saturated ketone absorption band (1723 cm^{-1}) prevailed on the carboxylic acid absorption band at 1711 cm^{-1}. This is a consequence of Norrish reactions, which only occur in photooxidation. The differences between photo- and thermooxidation are highlighted in Fig. 1g and 1h, which represent the deconvoluted spectra after 28 h of photooxidation and 270 h of thermooxidation.

As shown in Fig. 2a and 2b, different levels of oxidation were reached in thermo- and photooxidation. These results suggest that the bulk oxidation was higher under thermooxidative conditions than in photooxidative conditions, which reflects an oxidation profile in the case of photooxidation, confirmed when comparing the ATR-FTIR spectra of the front and rear surfaces of samples irradiated for 30 h or thermooxidized for 330 h (Fig. 1 i-j). In the case of thermooxidation, the rear side was practically as oxidized as the front, whereas in the case of photooxidation, it was significantly less oxidized. This heterogeneous oxidation results from a limited oxidation due to an oxygen starvation effect. A higher level of oxidation was observed in photooxidation. The surface oxidation is an important parameter to consider for biodegradation, as it will be colonized by microorganisms and will be one of the starting points of microbial attack.

The observed decrease of unsaturation (vinyl at 912 cm^{-1}, Fig. 2) was less for photooxidation. One should also consider that in the case of photooxidation, the photolysis of the ketones by Norrish type II reaction provokes the formation of vinyl double bonds (912 cm^{-1}). The loss of vinyl unsaturation is then, at least partially, compensated for by their formation.

3.1.3. Crosslinking and chain scission reactions

Besides the production of chemical moieties, oxidation reactions generate new chemical bonds or chain scissions. After each ageing time, the determination of gel fraction revealed the insoluble portion of SBR rapidly increased over the first 10 h of irradiation leading to a plateau of about 95 % (Fig. 2a). This increase can be evidenced even before the detection of any oxidation products by FTIR spectroscopy. In the case of thermooxidation, the gel fraction rose after 70 h and reached progressively a plateau of 80 % of insoluble after 300 h of ageing (Fig. 2b). Formation of this insoluble part reflects the creation of a network SBR structure through crosslinking reactions.

In addition, a decrease in the molecular weight of the samples was measured by size exclusion chromatography in the resulting soluble fraction, showing the occurrence of chain scissions under both conditions (Tables S1 and S2). These results indicated that the ratio of crosslinks to chain scissions are different depending on the ageing conditions and help us to understand the results of FTIR characterization. It was indeed observed that, as a result of photooxidation, the surface layers were quickly and strongly crosslinked, which decreased oxygen permeability, as previously reported by Adam et al. (Adam et al., 1990, 1989b). This contributed to the limitation of the photooxidation by the diffusion of oxygen, even in the case of this study where the thickness of the aged films is relatively weak (e=50 µm). Second, the absorbance of carbonylated products was limited to a plateau value of only 0.7. On the other hand, in the case of thermooxidation, with less crosslinking, the oxygen permeability is still sufficient to allow the bulk layer to be as oxidized as the front layer, as shown in Fig. 1h. The maximal value reached for the carbonyl absorbance measured by transmission spectroscopy was also much higher than for photooxidation. Our results and hypotheses agree with previous studies showing a decrease of the oxygen diffusion coefficient during the oxidation of SBR and polybutadiene, consistent with reduced oxygen permeability due to the rubber crosslinking (Clough and Gillen, 1992; Mertz et al., 2012; Sinturel and Billingham, 2000).

In any case, the oxidation processes induced significant transformations in the SBR network resulting in the formation of new covalent bonds in the degraded network, low molecular weight and highly functionalized products resulting from chain scissions. However, we are unable to discuss the environmental representativity of our results relative to a SBR from a full TRWP composition, as the oxidation state and crosslinking degree of SBR chains network within TRWP have not been reported yet. It can be expected that oxidation and scission/crosslinking reactions of vulcanized SBR in tire particles also occur in the environment (Cadle and Williams, 1980; Wagner et al., 2022). Indeed, the increase of the crosslinking density was already observed for unfilled SBR vulcanizates after photo-ageing (Karekar et al., 2023) and for carbon-black filled SBR vulcanizates after thermo-ageing (Rezig et al., 2020) but the characterization of short oxidized chains of SBR has never been reported.

3.1.4. Extraction and characterization of SBR short, oxidized chains

Short, oxidized chains resulting from chain scissions upon photo and thermooxidation could then be further leached out in aqueous solution as water-soluble products or remained in the films (surface and bulk) as extractable compounds. Pristine, 30 h photooxidized (SBR-photo-30h), 168 h and 330 h thermooxidized (SBR-thermo-168h and SBR-thermo-330h) SBR films were extracted in water and acetone to characterize qualitatively and quantitatively the leachable and extractable compounds, respectively.

3.1.4.1. Total organic carbon

Total organic carbon analysis was performed to evaluate the amount of such short chains released in the water and acetone and was expressed as a function of the oxidation level measured by ATR-FTIR at the surface of the sample (1720 cm^{-1}). Our results indicated that the amount of carbon in these extracts increased as a function of the surface oxidation level of SBR (Fig. 3). As expected, for pristine SBR, no extractable short, oxidized chain was detected either in water or in acetone (below the detection limit). For SBR-thermo-168h (low oxidized surface), short, oxidized chains were released as a small proportion (0.13 % and 3.65 % of total carbon in water and acetone, respectively). In contrast,

for the more oxidized samples (SBR-thermo-330h and SBR-photo-30h), a higher amount of carbon was released, in acetone especially. Proportions for photo and thermooxidation are equivalent. Leached products of SBR-thermo-330h and SBR-photo-30h represented 0.34 % and 0.47 % of the total carbon, respectively, whereas higher proportions (5.91 % and 5.46 %, respectively) were released in acetone extractable fractions. These results confirm the production of numerous short, oxidized chains under oxidative conditions and corroborate the decrease of molecular weight previously observed. Such water leachable and acetone extractable short chains could represent bioavailable substrates for bacteria. The combined fractions account for approximately 6 % of the total carbon (6 mg TOC out of 100 mg of the initial SBR-thermo-330h and SBR-photo-30h). The amount of short, oxidized chains was systematically higher in the acetone extract than in water indicating that such products constitute an intermediate pool of carbon between water soluble products and the insoluble fraction.

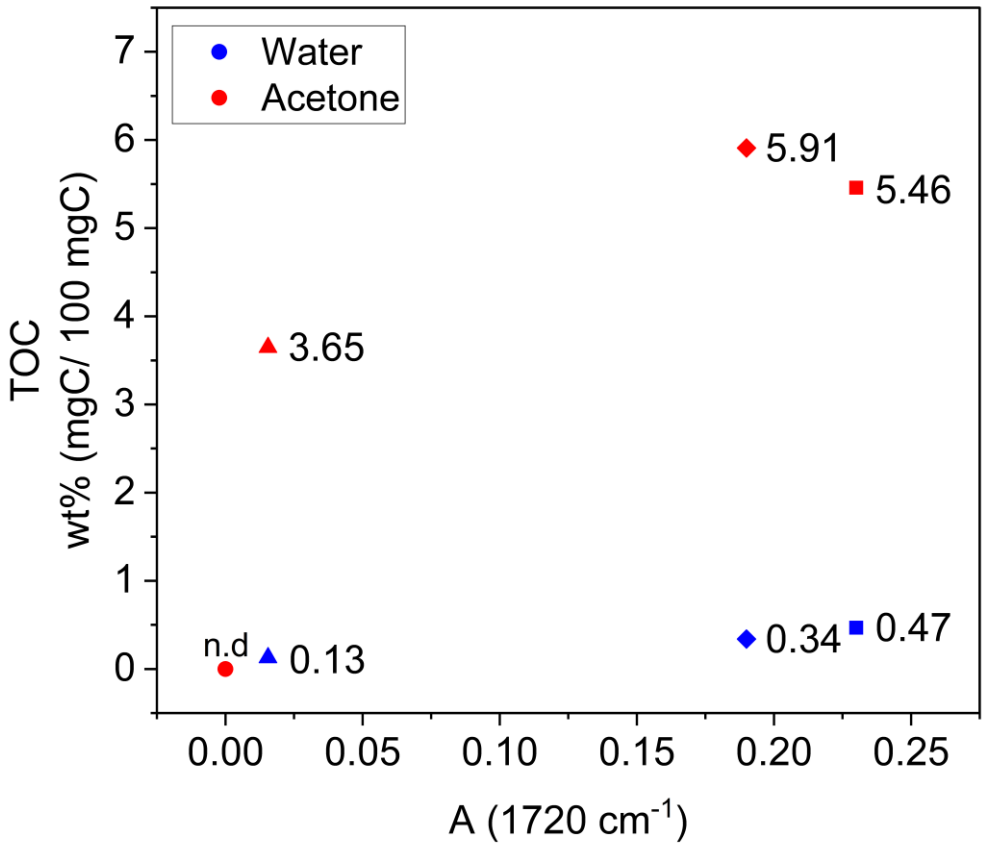

Fig. 3. Proportion of water (blue symbols) and acetone (red symbols) extracted short oxidized chains from SBR samples after 7-day extraction (wt% in mgC/ 100 mgC): pristine SBR (●), SBR-thermo-168h (▲), SBR-thermo-330h (◆) and SBR-photo-30h (■), determined by TOC measurements as a function of absorbance at 1720 cm^{-1} (carbonyl groups) at the surface of the films (FTIR-ATR). No carbon content was detected for the pristine SBR (n.d, below the detection limit).

3.1.4.2. ^{1}H NMR

The characterization of the short, oxidized chains resulting from chain scission and their quantification was complemented by ^{1}H NMR analysis. Specific profiles were obtained for each water and acetone extract of SBR sample and full spectrum integration was used to assess their relative abundance (Fig. S3). The results confirm the trends previously observed with TOC analyses showing an increase of the total amount of short, oxidized chains as a function of oxidation extent.

Besides this quantitative analysis, the ^{1}H NMR spectra provide a qualitative characterization of the different chemical structures of the SBR short, oxidized chains. Characteristic regions of the spectra were assigned to styrene aromatic protons (δ_H ~ 7.0-7.7 ppm in water; δ_H ~ 6.8-7.7 ppm in acetone), butadiene ethylenic protons (δ_H ~ 5.2-6.2 ppm in water; δ_H ~ 4.7-5.9 ppm in acetone) and aliphatic structures (δ_H ~ 0.7-3.2 ppm in water; δ_H ~ 0.7-2.8 ppm in acetone) (Fig. S3 and S4). Notably, the extracts exhibit high signals in the region of hydroxylated groups -OH (δ_H ~ 3.2-4.7 ppm) and low signals in the region of aldehyde protons —CHO (δ_H ~ 9.3-9.8 ppm in water; δ_H ~ 9.3-9.9 ppm in acetone), confirming that both leachable and extractable short chains contained oxidized moieties (Fig. S4). Structural assignment revealed more butadiene ethylenic protons in acetone extracts (20-30 % of total signal) than in water extracts (>10 % of total signal), confirming the extraction of longer aliphatic chains. On the contrary, the protons related to hydroxylated groups, represented 20 % and less than 10 % of total signal of water and acetone extracts, respectively. These results indicated that after abiotic degradation, short, oxidized chains can be released into water and

longer oxidized chains remained in the SBR films, as expected considering the effect of chain length on polarity and water solubility.

While studies on the characterization of leachable compounds are still scarce and mainly focus on chemical additives (Müller et al., 2022; Seuront et al., 2022), note that liquid ^{1}H NMR appears as a convenient tool to monitor the short oxidized chains that can be released after abiotic degradation, as already described for polyethylene (Eyheraguibel et al., 2017), polypropylene (Fontanella et al., 2013) or more recently polystyrene and polyethylene terephthalate (Giaganini et al., 2023). These short, oxidized chains produced and released in water can be considered as potential carbon substrates for microorganisms in the environment.

3.1.4.3. High resolution mass spectrometry

The characterization of the short, oxidized chains was finally completed with LC/HRMS analysis (examples of chromatograms are given in Fig. S5). For all samples, mass spectra showed a broad distribution of peaks in a mass range between 50 to 750 g.mol^{-1} (Fig. S6) but the composition of each spectrum varied in number of peaks and intensity. The water extracts were characterized by complex mass spectra consisting of hundreds of peaks (SBR-thermo-168h: 1645 peaks, SBR-thermo-330h: 1894 peaks, SBR-photo-30h: 1768 peaks) (Table 1). In the acetone extracts, a similar number of peaks was found for SBR-thermo-168h (1606 peaks), while 2400 peaks were detected for the high oxidized SBR-thermo-330h and 2523 for SBR-photo-30h. This large number of features reflected the diversity of the short, oxidized chains resulting from the oxidation and chain scission processes occurring during photo and thermooxidation. The extracts were characterized by an average molecular weight (Mw) of 326 and 352 g.mol^{-1} in water and up to 407 and 412 g.mol^{-1} in the acetone extracts for SBR-photo-30h and SBR-thermo-330h, respectively (Table 1). Previous studies on the abiotic degradation of polyethylene already reported similar molecular weight ranges and number of peaks, indicating that abiotic oxidation leads to the production of small compounds lower than 1000 Da (Eyheraguibel et al., 2018, 2017). These short oxidized chains must be considered as potential

substrates in addition to the uncrosslinked and crosslinked SBR chains resulting from abiotic ageing. So far, very few studies focused on SBR degradation products. Only recently, Thomas et al. (2022) proposed a list of possible transformation products of elastomer resulting from thermal or photo-ageing of tire cryogrinds. Oxidation products such as carboxylic acids, ketones and epoxides were detected in THF extract by GC/MS, but few compounds could be identified through targeted approach as no database provides a comprehensive list of degradation products. In this study, Van Krevelen diagrams (VKD) were used to better visualize and understand the complex chemical composition of the extracts (Fig. 4a and 4b). Specific regions of the diagram provide information on alkylation and oxidation of the compounds. The most oxidized compounds have high O/C ratios (> 0.5) and appear on the right side of the plot. Aliphatic compounds typically have high H/C ratios (> 1.5) and low O/C ratios (< 0.5) and aromatic hydrocarbons have low H/C ratios (< 1.0) and O/C ratios (< 0.5) and appear respectively in the upper left and lower left part of the diagram (Kim et al., 2003; Kourtchev et al., 2014; Noziere et al., 2015). On the Fig. 4a and 4b, four regions were defined to represent (1) highly unsaturated compounds, (2) intermediately oxidized, (3) highly oxidized and (4) very highly oxidized according to Sueur et al. (2023). The distribution of the short, oxidized chains was similar for both ageing and extracting conditions with a wider distribution of compounds in acetone extract (Fig. 4b) corresponding to a higher number of peaks detected. The VKD showed that random chain scissions occurred producing mixed short, oxidized chains containing all the aromatic/unsaturated, aliphatic, and oxidized moieties present originally in the chemical structure of the SBR monomers (Fig. S4). The most represented compounds contained unsaturated moieties (region 1) attributed to styrene and diene bonds. Intermediately oxidized compounds (region 2) were present in both water and acetone extracts in large quantity while highly and very highly oxidized compounds (regions 3 and 4) appeared with a larger amount in acetone extract, reflecting the advanced oxidation level of the surface and bulk film. Further work will be required to identify these short, oxidized chains.

Table 1. Characteristics of SBR water (supernatant) and acetone extracted short, oxidized chains and residue after 30-day incubation with *R. ruber* (RR), *G. polyisoprenivorans* (GP) or without bacteria (abiotic control (AB)). nd = non-detected. The mean values (n=2 ± SD) of gel fraction are presented.

Materials		SBR	SBR-thermo-168h			SBR-thermo-330h			SBR-photo-30h		
Sample			AB	RR	GP	AB	RR	GP	AB	RR	GP
Number of peaks	Water	nd	1645	654	1035	1894	1500	1511	1768	1105	1550
	Acetone	nd	1606	1007	1355	2400	2113	1389	2523	2390	1488
Mw ($g.mol^{-1}$)	Water	nd	323	317	344	352	341	352	326	335	346
	Acetone	nd	333	387	416	412	413	418	407	401	406
Gf	%	0	35±7	19±2	44±3	80±4	87±3	89±9	81±1	89±1	88±3

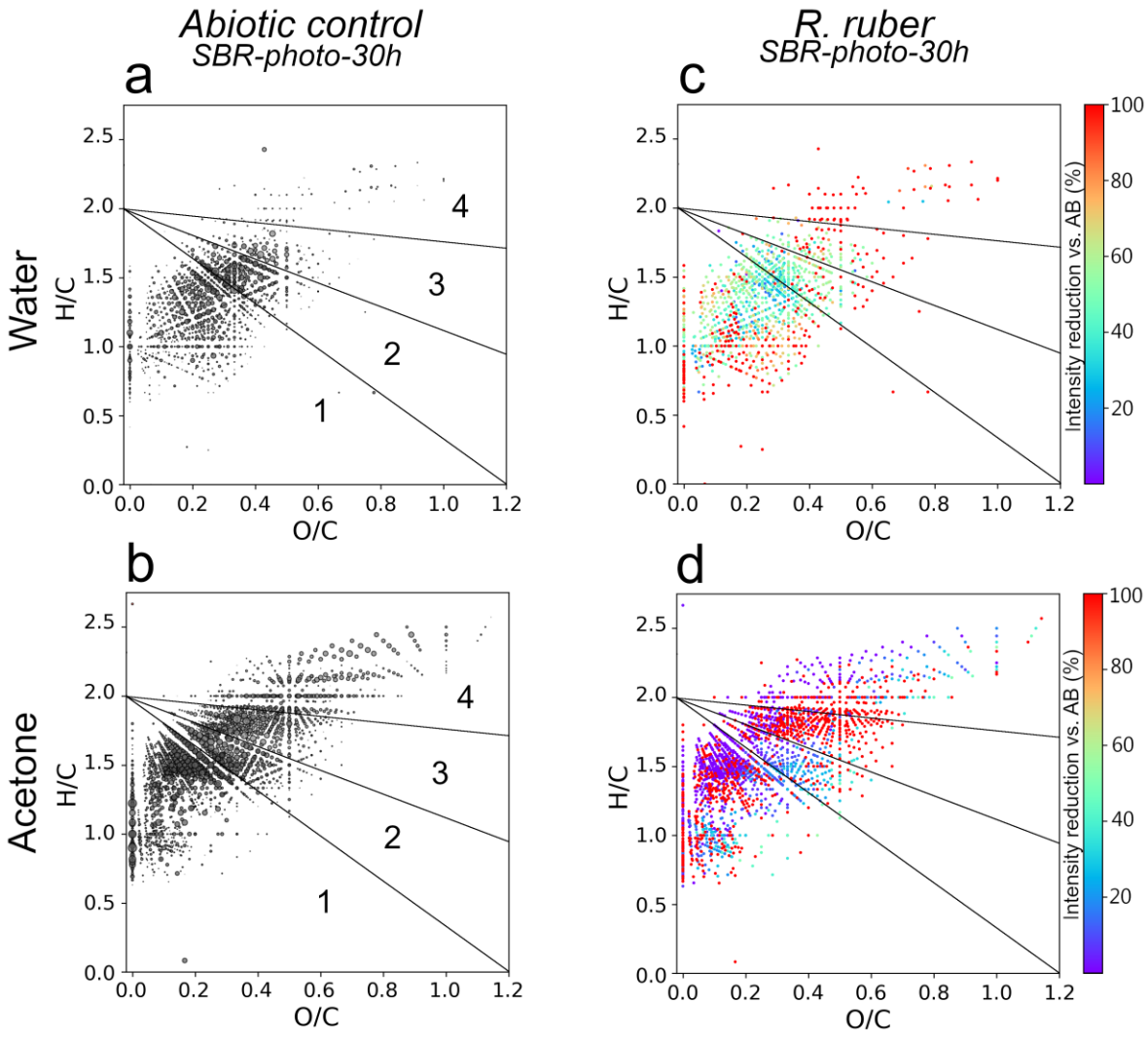

Fig. 4. Van Krevelen diagrams of LC/MS ESI (+) data showing **on the left column**, the H/C vs. O/C atomic ratio for compounds in the water (a) and acetone (b) extract of the SBR-photo-30h abiotic control (AB). Point size represents the peak intensity. They are separated in 4 regions: (1) highly unsaturated compounds, (2) intermediately oxidized, (3) highly oxidized and (4) very highly oxidized; **on the right column**, the degradation of compounds (peak intensity reduction (%)) in the water (supernatant) (c) and acetone (d) extract of SBR-photo-30h after a 30-day incubation with *R. ruber*. Intensities above 10^4 were considered. The level of degradation is represented by a color scale from fully degraded (red) to not degraded (purple).

3.2. Biotic degradation

3.2.1. Bacterial growth

The biodegradation of pristine and photo- or thermooxidized SBR films by two bacterial strains, *R. ruber* and *G. polyisoprenivorans*, was investigated. For a given SBR sample, similar growth was observed with both strains, but the rate of biodegradation (% ThOD, SI equation 1) increased with the level of SBR oxidation (Fig. 5a). The lowest biodegradation percentage was observed for pristine SBR (less than 0.1 % for both strains) and a slight increase was observed for SBR-thermo-168h (0.2 %) after 30 days of incubation. Higher biodegradation percentages were obtained with more oxidized samples, up to 0.5-1 % with SBR-thermo-330h and up to 1.2 % with SBR-photo-30h. For each pre-oxidized SBR, the bacterial growth started immediately and kept rising for 30 days without reaching a plateau. Although growth curves for both strains were similar for most SBR samples, a significant difference was observed for SBR-thermo-330h, showing a higher biodegradation capacity of *R. ruber* in this case. The measurement of the ATP content confirmed these trends and clearly showed the production of more biomass with pristine and oxidized SBR, compared to the control, reflecting the variable bacterial growth (Fig. 5b). A slight increase of ATP amount was measured for pristine SBR suggesting a minimal bacterial growth within the timeframe of the experiment. The amount of ATP was much higher when bacteria were cultivated on more oxidized samples, except for the condition *R.*

ruber / SBR-thermo-168h. Globally, the oxidation (photo and thermo) of SBR promoted both mineralization and biomass production.

Both strains were isolated from the environment and appeared as newly identified degraders of photo and thermooxidized SBR. The biodegradation capacity of *R. ruber* has already been reported in the literature on various pre-oxidized polymers such as polyethylene (Bonhomme et al., 2003; Eyheraguibel et al., 2017), polypropylene (Fontanella et al., 2013) and more recently, extractable SBR from environmental aged roadway particles (Calarnou et al., 2023). Our results confirmed that *R. ruber* can degrade pre-oxidized SBR as the sole carbon source. So far, there is no evidence of bacterial growth on similar oxidized SBR samples. Only a few studies reported bacterial isolates able to grow on vulcanized SBR (ground tire rubber) such as *Acidithiobacillus ferroxidans*, *Gordonia* sp. and *Sphingomonas* sp., in a context of devulcanization and recycling (Cui et al., 2016; Li et al., 2013). Tsuchii et al. also reported that unvulcanized SBR and BR were hardly attacked by *Nocardia* sp. and *Moraxella* sp. (Tsuchii et al., 1985, 1984). The authors indicated that only BR samples with an average molecular weight of 2,500 or less were degraded and assimilated by *Moraxella* sp. in 5 days (Tsuchii et al., 1984). This observation supports our results which showed that the low molecular weight generated in pre-oxidized SBR samples (soluble fraction of THF) might enhance biodegradation.

In our study, complementary control experiments carried out on IR substrate provided different results for the two strains tested. The biodegradation percentage obtained with *G. polyisoprenivorans* on IR reached 3% within the first 20 days and levelled off until the end of the experiment probably due to the limiting oxygen in the system (Fig. S7). The biomass production (ATP) exceeded the level of the biotic control 28-fold, and at least 5-fold that of oxidized SBR samples, exhibiting significantly higher growth on IR for this strain (Fig. 5c). Such results were expected as *G. polyisoprenivorans* VH2 is a well-known bacterium able to degrade IR with high biodegradation rates (20 % of mineralization in 50 days) (Andler et al., 2018; Linos and Steinbüchel, 1998; Warneke et al., 2007). Interestingly, they also point out that *G. polyisoprenivorans* biodegrade pristine SBR, pristine IR and oxidized SBR at various rates and suggest that different mechanisms of

degradation could occur according to the material. Moreover, no increase in bacterial growth or ATP content was recorded for *R. ruber* with IR, suggesting that metabolic pathways involved in the biodegradation of oxidized SBR were not effective for the degradation of IR. These results emphasize the capacity of each strain to grow on aged SBR and the need to perform further research to elucidate their mechanisms of biodegradation.

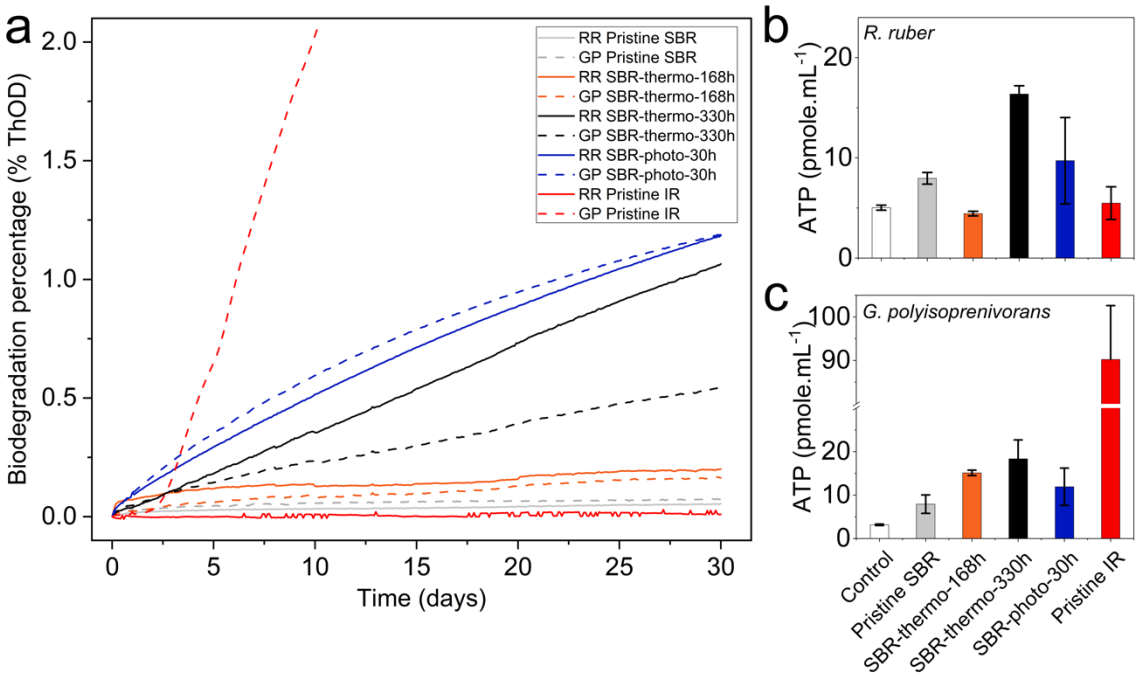

Fig. 5. Bacterial growth (biodegradation kinetics **(a,** % ThOD**)** and total ATP content **(b, c)**) of *R. ruber* (solid lines, b) and *G. polyisoprenivorans* (dashed lines, c) cultivated on pristine SBR (grey), SBR-thermo-168h (orange), SBR-thermo-330h (black), SBR-photo-30h (blue) and pristine IR (red) or without any carbon source (Control) for 30 days. The mean values (n=2 ± SD) are presented.

3.2.2. Evaluation of biodegradation by ^{1}H NMR spectroscopy

At the end of the biodegradation experiment (30 days of incubation), the consumption of short, oxidized chains as potential bioavailable carbon sources was assessed by comparing the ^{1}H NMR signal intensities of each sample to the abiotic control (Fig. 6a). The water extractable products recorded a 25-50 % decrease of the signal intensity for SBR-thermo-330h and SBR-photo-30h

samples and reached more than 75 % for the SBR-thermo-168h after 30 days of culture (Fig. 6b). Similarly, the signal intensity of acetone extracts decreased from 30 % to 43 % for SBR-photo-30h and SBR-thermo-330h samples but no decrease was observed for SBR-thermo-168h (Fig. 6c). Moreover, no significant difference in the relative proportion of the previously assigned region was observed, suggesting that removal (either by bacterial uptake or enzymatic transformation) did not target any preferential chemical structure (Fig. S8, S9 and S10). The results suggested the bioassimilation of the short, oxidized chains instead, and indicated that the strains can use both compounds leached out in the supernatant and the extractables remaining in the oxidized films. The consumption of the acetone extracted compounds could suggest an adhesive growth of both bacteria. Indeed, the *Rhodococcus* and *Gordonia* genera were already reported as adhesive bacteria on rubber substrates (Basik et al., 2021; Chengalroyen and Dabbs, 2013) and their development at the surface of rubber was already observed by scanning electron microscopy (SEM) (Andler et al., 2022; Berekaa et al., 2000).

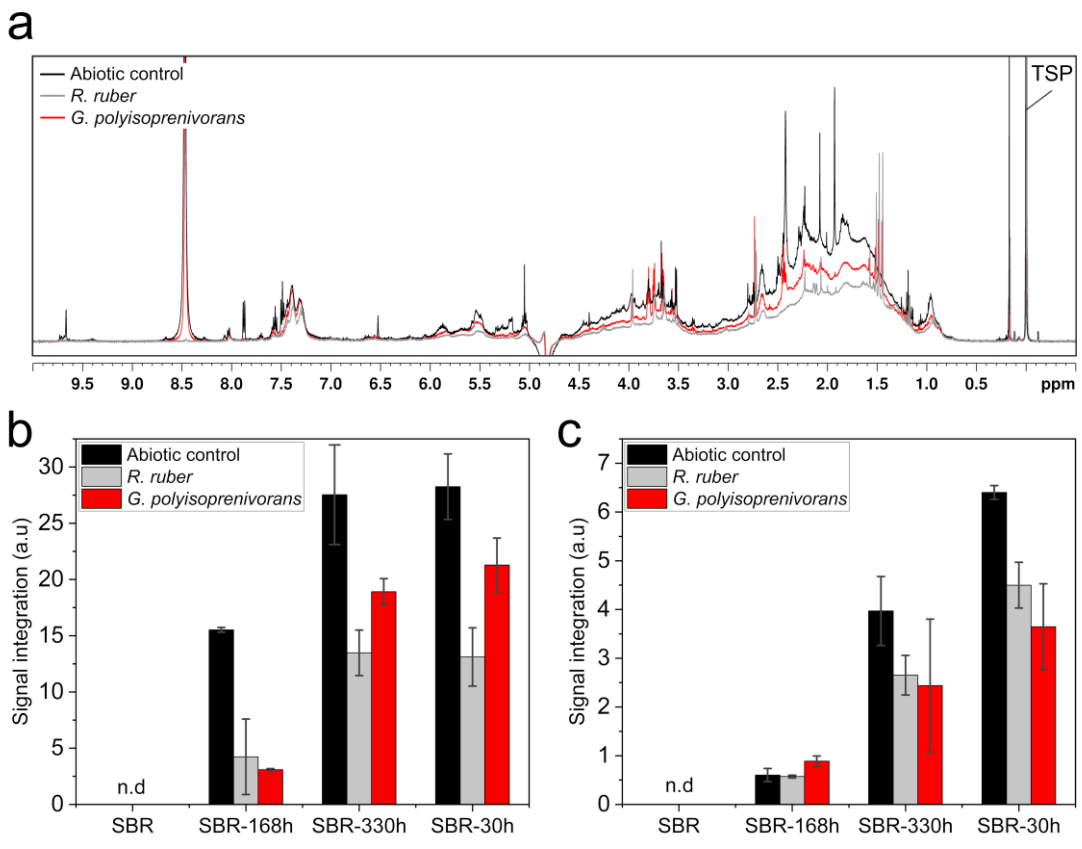

584 **Fig. 6**. **(a)** ^{1}H NMR spectra of the SBR-photo-30h supernatants obtained with *R. ruber* (grey), *G.*
585 *polyisoprenivorans* (red) and without bacteria (abiotic control) (black) after 30-day incubation. For a
586 better visualization, only one replicate is presented on the figure. NMR relative integrations (arbitrary
587 unit) of water-soluble (supernatant) **(b)** and acetone **(c)** extracted short, oxidized chains with *R. ruber*
588 (grey bars), *G. polyisoprenivorans* (red bars) or without bacteria (abiotic control) (black bars). No
589 signal was detected for the pristine SBR (n.d). Arbitrary units (a.u) are not comparable between water
590 and acetone analyses as the internal standard used was different. The mean values (n=2 ± SD) are
591 presented.

592

593 *3.2.3. Evaluation of biodegradation by mass spectrometry*

594 After the biodegradation experiment, the number of peaks detected by mass spectrometry decreased in
595 different proportions according to the SBR extract analyzed (Table 1), revealing that 6 % to 60 % of
596 compounds were completely biodegraded. Van Krevelen diagrams were plotted using a color scale
597 from red (fully degraded) to purple (no degradation) to monitor the evolution of the short, oxidized
598 chain composition in the water (supernatants) and acetone extracts of SBR-photo-30h (Fig. 4c-d and
599 S11), SBR-thermo-330h (Fig. S12 and S13) and SBR-thermo-168h (Fig. S14 and S15). In the
600 presence of *R. ruber* and *G. polyisoprenivorans*, numerous compounds were highly or partly degraded
601 in both water and acetone extracts (red dots). This confirmed that biodegradation of short, oxidized
602 chains can occur in the medium and at the surface of the films. The average molecular weight of
603 remaining short, oxidized chains did not change indicating the degradation of compounds with sizes
604 from 50 up to 750 $g.mol^{-1}$ (Table 1). Moreover, all the different classes of compounds were impacted
605 showing that the chemical structure of the oxidized chains did not limit biodegradation. However,
606 aromatic compounds (region 1 - H/C ratios <1.0) seemed more degraded than aliphatic ones (region 1
607 - H/C ratios >1.5) while highly oxidized molecules (regions 3 and 4) were strongly degraded (Fig. 4c
608 and 4d). These results did not allow us to conclude that there is a preferential degradation of a
609 chemical structure.

610

3.2.4. Evolution of the insoluble fraction of SBR

After abiotic degradation, the insoluble crosslinked SBR fraction and THF soluble fraction could also be a potential carbon resource for bacteria as it represented 35 % of the carbon of SBR-thermo-168h samples and 80 % on average for the most oxidized SBR-thermo-330h and SBR-photo-30h samples (Table 1). At the end of biodegradation experiments, the insoluble fraction of SBR-thermo-330h and SBR-photo-30h tends to increase by 10 % on average in the presence of both strains compared to the abiotic control (Table 1), suggesting a concomitant reduction of the THF soluble fraction. This increase even reached 25 % for SBR-thermo-168h with *G. polyisoprenivorans*. Combined with the mass spectrometry data, these results might suggest that no or low degradation or cleavage of the insoluble fraction occurred within the 30 days of culture and longer incubation times must be tested to conclude on the use of the crosslinked network as a carbon substrate. As expected, the short oxidized chains biodegraded faster than the high molecular weight crosslinked chains, as reported for BR (Tsuchii et al., 1984). On the other hand, the THF soluble fraction of the residual film was clearly degraded by the two strains, indicating that biodegradation processes take place on several carbon sources. Conversely, the SBR-thermo-168h insoluble fraction percentage with *R. ruber* is almost halved. This surprising result could suggest a partial attack of the insoluble residue as moreover, a high biodegradation level of the soluble short, oxidized chain compounds was also observed with this strain (-60 % and -37 % of the number of peaks detected by mass spectrometry in the supernatant and in the acetone extract after biodegradation, respectively, (Table 1) with a high biodegradation percentage (Fig. S14). Nevertheless, these results do not match with those obtained for biological parameters, the BOD-based biodegradation percentage and ATP content for *R. ruber* remaining low (Fig. 5). As for the other samples, longer incubation time must be tested to conclude on the use of the crosslinked network as a carbon substrate.

3.2.5. Extracellular protein content

Previous works have shown the key role of extracellular enzymes to attack polymer surface and released oligomers (Chow et al., 2022; Hiessl et al., 2012; Jendrossek, 2019; Odobel et al., 2021;

638 Santo et al., 2013). Therefore, protein amount in the supernatant was measured for the different
639 samples. The protein content increased with the level of oxidation of the SBR samples. The lowest
640 protein content (6 µg.mL^{-1}) was observed in SBR-thermo-168h supernatant while higher contents were
641 measured in the case of SBR-thermo-330h (16 µg.mL^{-1}) and SBR-photo-30h (20-23 µg.mL^{-1}) for both
642 strains (Fig. 7). Similarly, the protein content was positively correlated with the level of consumption
643 of short, oxidized chains. It would now be interesting to assess whether these proteins correspond to
644 enzymes potentially involved in the degradation of SBR material or the cleavage of oxidized chains to
645 enhance their assimilation. To date, strong focus was more on extracellular oxidative enzymes
646 efficient towards IR and NR. Indeed, some enzymes were reported in the literature to cleave C=C
647 bonds of polyisoprene such as peroxidase and laccase (Cheng et al., 2023), latex clearing protein
648 (Hiessl et al., 2014), rubber oxygenases RoxA and RoxB (Birke et al., 2017; Jendrossek and
649 Reinhardt, 2003). In our positive control experiment, a strong growth of *G. polyisoprenivorans* was
650 observed on IR and the extracellular protein measurement reached 26 µg.mL^{-1} (Fig. 7) probably
651 reflecting the production of $Lcp1_{VH2}$ and $Lcp2_{VH2}$ enzymes as described in the literature (Andler, 2020;
652 Andler and Steinbüchel, 2017; Hiessl et al., 2014). Low extracellular protein contents were detected in
653 the presence of pristine SBR, suggesting an absence of enzymatic activity on the non-oxidized SBR.
654 On the contrary, high level of extracellular proteins (23 µg.mL^{-1}) was measured in the supernatant of
655 *G. polyisoprenivorans* growing on oxidized SBR. but further analyses are required to confirm the
656 presence of enzymes and test their potential activity on oxidized SBR.

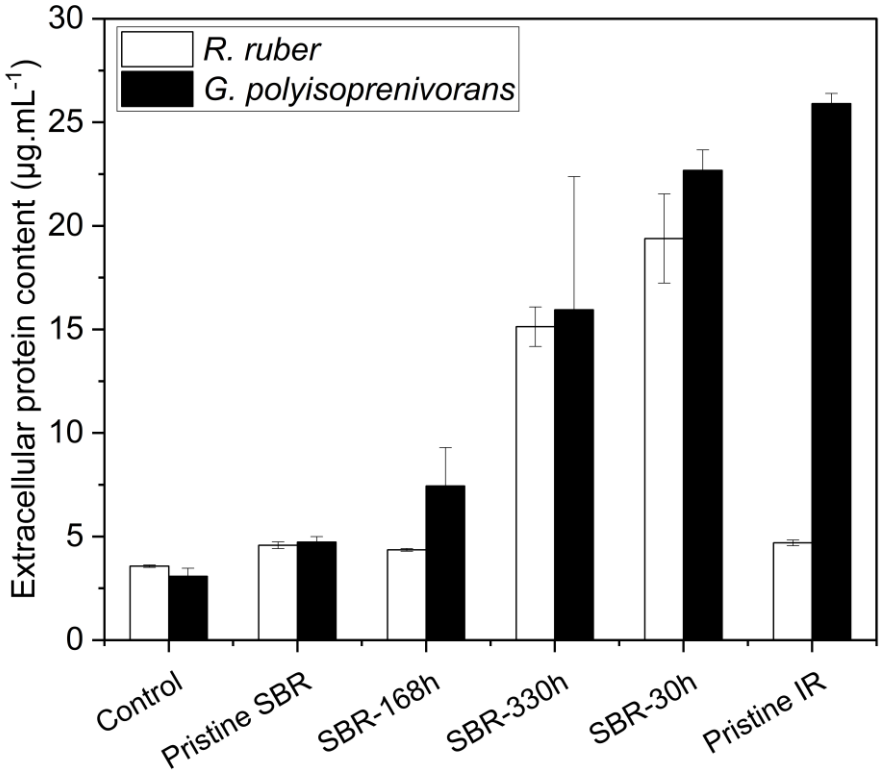

Fig. 7. Extracellular protein content (Bradford assay) in supernatants of *R. ruber* and *G. polyisoprenivorans* cultivated 30 days in the presence of pristine SBR, SBR-thermo-168h, SBR-thermo-330h, SBR-photo-30h or pristine IR. The mean values (n=2 ± SD) are presented.

3.3 Limitation of environmental model research: pristine SBR degradation to represent TRWP?

As a major component of tire tread, SBR undergoes various stresses during the tire use phase and after its emission into the environment in TRWP. The purpose of this work was to study a simplified system (pristine SBR) to overcome the complexity of TRWP composition and focus on the mechanisms underlying the degradation of SBR. This first step highlighted that the aging of a pure SBR induced significant transformations of the elastomer via oxidation processes. The formation of new covalent bonds resulted in a crosslinked SBR network, while chain scissions concurrently led to the formation of low molecular weight and highly functionalized products, that can then be biodegraded. Nevertheless, our model system will need to be progressively complexified to more realistically mimic

the fate of the elastomer phase within TRWP in an environmental context and to understand what will impact its biodegradation: vulcanization, elastomer microstructure and the presence of other components embedded in TRWP (fillers, plasticizers, protective and vulcanizing agents) should especially be considered for future studies.

4. Conclusion

The present study provides new insights about the abiotic degradation of SBR and its impact on biodegradation. Under abiotic conditions, photo or thermo-oxidation processes lead to the production of multiple compounds, mainly short, oxidized chains resulting from main chain scissions and containing high amount of unsaturation and carbonylated functions. These short chains can be released in the water phase to become potential substrates for microorganisms. Further investigations are now required to identify their chemical composition.

The capacity of two strains, *Rhodoccocus ruber* and *Gordonia polyisoprenivorans*, to grow on weathered SBR material was demonstrated for the first time. Different carbon sources were considered for biodegradation such as the short, oxidized chains and the crosslinked matrix resulting from abiotic degradation. Our results indicate that both strains were able to degrade the low molecular weight oxidized SBR but not the pristine SBR. These results evidence the positive impact of abiotic degradation on the biodegradation process. It would now be interesting to check whether this biodegradation requires the action of specific bacteria such as *Rhodoccocus ruber* and *Gordonia polyisoprenivorans*, or could be observed with other strains or microbial consortia. The high extracellular protein content, measured when the strains were grown on highly oxidized SBR samples, raised questions about the potential involvement of enzymatic activities toward the SBR material or its abiotic degradation product (short, oxidized chains). Further investigations are in progress in our laboratory.

Acknowledgements

All NMR analyses were performed within the MetaboHUB French infrastructure (ANR-INBS-0010).

References

Aboelkheir, M.G., Bedor, P.B., Leite, S.G., Pal, K., Toledo Filho, R.D., Gomes de Souza, F., 2019. Biodegradation of Vulcanized SBR: A Comparison between *Bacillus subtilis*, *Pseudomonas aeruginosa* and *Streptomyces* sp. Sci. Rep. 9, 1–12. https://doi.org/10.1038/s41598-019-55530-y

Adam, C., Lacoste, J., Lemaire, J., 1990. Photo-oxidation of elastomeric materials: Part IV-Photo-oxidation of 1,2-polybutadiene. Polym. Degrad. Stab. 29, 305–320. https://doi.org/10.1016/0141-3910(90)90042-6

Adam, C., Lacoste, J., Lemaire, J., 1989a. Photo-oxidation of elastomeric materials: Part II-Photo-oxidation of styrene-butadiene copolymer. Polym. Degrad. Stab. 26, 269–284. https://doi.org/10.1016/0141-3910(89)90079-7

Adam, C., Lacoste, J., Lemaire, J., 1989b. Photo-oxidation of elastomeric materials. Part l-Photo-oxidation of polybutadienes. Polym. Degrad. Stab. 24, 185–200. https://doi.org/10.1016/0141-3910(89)90091-8

Albertsson, A.C., Karlsson, S., 1990. The influence of biotic and abiotic environments on the degradation of polyethylene. Prog. Polym. Sci. 15, 177–192. https://doi.org/10.1016/0079-6700(90)90027-X

Andler, R., 2020. Bacterial and enzymatic degradation of poly(cis-1,4-isoprene) rubber: Novel biotechnological applications. Biotechnol. Adv. 44, 107606. https://doi.org/10.1016/j.biotechadv.2020.107606

Andler, R., Guajardo, C., Sepúlveda, C., Pino, V., Sanhueza, V., D'Afonseca, V., 2022. Biodegradation of rubber in cultures of *Rhodococcus rhodochrous* and by its enzyme latex clearing protein. Biodegradation 33, 609–620. https://doi.org/10.1007/s10532-022-09998-7

Andler, R., Hiessl, S., Yücel, O., Tesch, M., Steinbüchel, A., 2018. Cleavage of poly(cis-1,4-isoprene) rubber as solid substrate by cultures of *Gordonia polyisoprenivorans*. N. Biotechnol. 44, 6–12.

https://doi.org/10.1016/j.nbt.2018.03.002

Andler, R., Steinbüchel, A., 2017. A simple, rapid and cost-effective process for production of latex clearing protein to produce oligopolyisoprene molecules. J. Biotechnol. 241, 184–192. https://doi.org/10.1016/j.jbiotec.2016.12.008

Babbit, O.R., 2010. The Vanderbilt Rubber Handbook, 14th ed. R. T. Vanderbilt Company.

Baensch-Baltruschat, B., Kocher, B., Kochleus, C., Stock, F., Reifferscheid, G., 2021. Tyre and road wear particles - A calculation of generation, transport and release to water and soil with special regard to German roads. Sci. Total Environ. 752, 141939. https://doi.org/10.1016/j.scitotenv.2020.141939

Baensch-Baltruschat, B., Kocher, B., Stock, F., Reifferscheid, G., 2020. Tyre and road wear particles (TRWP) - A review of generation, properties, emissions, human health risk, ecotoxicity, and fate in the environment. Sci. Total Environ. 733, 137823. https://doi.org/10.1016/j.scitotenv.2020.137823

Basik, A., Sanglier, J.-J., Yeo, C., Sudesh, K., 2021. Microbial Degradation of Rubber: Actinobacteria. Polymers (Basel). 13, 1989. https://doi.org/10.3390/polym13121989

Baumann, W., Ismeier, M., 1998. Kautschuk und Gummi - Daten und Fakten zum Umweltschutz., First. ed. Springer Verlag, Berlin Heidelberg. https://doi.org/https://doi.org/10.1007/978-3-642-58916-4.

Berekaa, M.M., 2006. Colonization and microbial degradation of polyisoprene rubber by nocardioform actinomycete *Nocardia* sp. strain-MBR. Biotechnology 5, 234–239. https://doi.org/10.3923/biotech.2006.234.239

Berekaa, M.M., Linos, A., Reichelt, R., Keller, U., Steinbüchel, A., 2000. Effect of pretreatment of rubber material on its biodegradability by various rubber degrading bacteria. FEMS Microbiol. Lett. 184, 199–206. https://doi.org/10.1111/j.1574-6968.2000.tb09014.x

Birke, J., Röther, W., Jendrossek, D., 2017. RoxB is a novel type of rubber oxygenase that combines

properties of rubber oxygenase RoxA and latex clearing protein (Lcp). Appl. Environ. Microbiol. 83, e00721-17. https://doi.org/10.1128/AEM.00721-17

Bode, H.B., Zeeck, A., Pluckhahn, K., Jendrossek, D., 2000. Physiological and chemical investigations into microbial degradation of synthetic poly(cis-1,4-isoprene). Appl. Environ. Microbiol. 66, 3680–3685. https://doi.org/10.1128/AEM.66.9.3680-3685.2000

Bonhomme, S., Cuer, A., Delort, A.M., Lemaire, J., Sancelme, M., Scott, G., 2003. Environmental biodegradation of polyethylene. Polym. Degrad. Stab. 81, 441–452. https://doi.org/10.1016/S0141-3910(03)00129-0

Borel, M., Kergomard, A., Renard, M.F., 1982. Degradation of natural rubber by fungi imperfecti. Agric. Biol. Chem. 46, 877–881. https://doi.org/10.1080/00021369.1982.10865189

Cadle, S.H., Williams, R.L., 1980. Environmental Degradation of Tire Wear Particles. Rubber Chem. Technol. 53, 903–914. https://doi.org/10.5254/1.3535066

Calarnou, L., Traïkia, M., Leremboure, M., Malosse, L., Dronet, S., Delort, A.M., Besse-Hoggan, P., Eyheraguibel, B., 2023. Assessing biodegradation of roadway particles via complementary mass spectrometry and NMR analyses. Sci. Total Environ. 900, 165698. https://doi.org/10.1016/j.scitotenv.2023.165698

Chandra, R., 1983. Protection of styrene-butadiene copolymer film with bound synergistic stabilizers against ferric stearate - catalysed photo-oxidative degradation at elevated temperature. Polymer (Guildf). 24, 229–233. https://doi.org/10.1016/0032-3861(83)90138-6

Cheng, X., Xia, M., Yang, Y., 2023. Biodegradation of vulcanized rubber by a gut bacterium from plastic-eating mealworms. J. Hazard. Mater. 448, 130940. https://doi.org/10.1016/j.jhazmat.2023.130940

Chengalroyen, M.D., Dabbs, E.R., 2013. The Biodegradation of Latex Rubber: A Minireview. J. Polym. Environ. 21, 874–880. https://doi.org/10.1007/s10924-013-0593-z

Chow, J., Perez-Garcia, P., Dierkes, R., Streit, W.R., 2022. Microbial enzymes will offer limited

775 solutions to the global plastic pollution crisis. Microb. Biotechnol. 16, 195–217.
776 https://doi.org/10.1111/1751-7915.14135

777 Clough, R.L., Gillen, K.T., 1992. Oxygen diffusion effects in thermally aged elastomers. Polym.
778 Degrad. Stab. 38, 47–56. https://doi.org/10.1016/0141-3910(92)90022-W

779 Corti, A., Muniyasamy, S., Vitali, M., Imam, S.H., Chiellini, E., 2010. Oxidation and biodegradation
780 of polyethylene films containing pro-oxidant additives: Synergistic effects of sunlight exposure,
781 thermal aging and fungal biodegradation. Polym. Degrad. Stab. 95, 1106–1114.
782 https://doi.org/10.1016/j.polymdegradstab.2010.02.018

783 Cui, X., Zhao, S., Wang, B., 2016. Microbial desulfurization for ground tire rubber by mixed
784 consortium-*Sphingomonas* sp. and *Gordonia* sp. Polym. Degrad. Stab. 128, 165–171.
785 https://doi.org/10.1016/j.polymdegradstab.2016.03.011

786 Eyheraguibel, B., Leremboure, M., Traikia, M., Sancelme, M., Bonhomme, S., Fromageot, D.,
787 Lemaire, J., Lacoste, J., Delort, A.M., 2018. Environmental scenarii for the degradation of oxo-
788 polymers. Chemosphere 198, 182–190. https://doi.org/10.1016/j.chemosphere.2018.01.153

789 Eyheraguibel, B., Traikia, M., Fontanella, S., Sancelme, M., Bonhomme, S., Fromageot, D., Lemaire,
790 J., Lauranson, G., Lacoste, J., Delort, A.M., 2017. Characterization of oxidized oligomers from
791 polyethylene films by mass spectrometry and NMR spectroscopy before and after biodegradation
792 by a *Rhodococcus rhodochrous* strain. Chemosphere 184, 366–374.
793 https://doi.org/10.1016/j.chemosphere.2017.05.137

794 Fohet, L., Andanson, J.M., Charbouillot, T., Malosse, L., Leremboure, M., Delor-Jestin, F., Verney,
795 V., 2023. Time-concentration profiles of tire particle additives and transformation products under
796 natural and artificial aging. Sci. Total Environ. 859, 160150.
797 https://doi.org/10.1016/j.scitotenv.2022.160150

798 Fontanella, S., Bonhomme, S., Brusson, J.M., Pitteri, S., Samuel, G., Pichon, G., Lacoste, J.,
799 Fromageot, D., Lemaire, J., Delort, A.M., 2013. Comparison of biodegradability of various

polypropylene films containing pro-oxidant additives based on Mn, Mn/Fe or Co. Polym. Degrad. Stab. 98, 875–884. https://doi.org/10.1016/j.polymdegradstab.2013.01.002

Giaganini, G., Cifelli, M., Biagini, D., Ghimenti, S., Corti, A., Castelvetro, V., Domenici, V., Lomonaco, T., 2023. Multi-Analytical Approach to Characterize the Degradation of Different Types of Microplastics: Identification and Quantification of Released Organic Compounds. Molecules 28, 1382. https://doi.org/10.3390/molecules28031382

Goßmann, I., Halbach, M., Scholz-Böttcher, B.M., 2021. Car and truck tire wear particles in complex environmental samples – A quantitative comparison with "traditional" microplastic polymer mass loads. Sci. Total Environ. 773, 145667. https://doi.org/10.1016/j.scitotenv.2021.145667

Hiessl, S., Böse, D., Oetermann, S., Eggers, J., Pietruszka, J., Steinbüchel, A., 2014. Latex clearing protein-an oxygenase cleaving poly(cis-1,4-isoprene) rubber at the cis double bonds. Appl. Environ. Microbiol. 80, 5231–5240. https://doi.org/10.1128/AEM.01502-14

Hiessl, S., Schuldes, J., Thürmer, A., Halbsguth, T., Bröker, D., Angelov, A., Liebl, W., Daniel, R., Steinbüchel, A., 2012. Involvement of two latex-clearing proteins during rubber degradation and insights into the subsequent degradation pathway revealed by the genome sequence of *Gordonia polyisoprenivorans* strain VH2. Appl. Environ. Microbiol. 78, 2874–2887. https://doi.org/10.1128/AEM.07969-11

Hu, M., Zhao, S., Li, C., Wang, B., Fu, Y., Wang, Y., 2016. Biodesulfurization of vulcanized rubber by enzymes induced from *Gordonia amicalisa*. Polym. Degrad. Stab. 128, 8–14. https://doi.org/10.1016/j.polymdegradstab.2016.02.017

Hu, X., Zhao, H.N., Tian, Z., Peter, K.T., Dodd, M.C., Kolodziej, E.P., 2022. Transformation Product Formation upon Heterogeneous Ozonation of the Tire Rubber Antioxidant 6PPD (N-(1,3-dimethylbutyl)- N′-phenyl- p-phenylenediamine). Environ. Sci. Technol. Lett. 9, 413–419. https://doi.org/10.1021/acs.estlett.2c00187

Ibrahim, E.M.A., El-ameen, T.M., 2013. Degradation of natural and synthetic rubber by *Gordonia*

alkanivorans strain E1. J. Agric. Chem. Biotechnol. 4, 17–28. https://doi.org/10.21608/jacb.2013.52994

ISO 14851, 2019. Determination Of The Ultimate Aerobic Biodegradability Of Plastic Materials In An Aqueous Medium - Method By Measuring The Oxygen Demand In A Closed Respirometer (ISO 14851:2019).

Jecusco, F.P., 1926. The Addition of Light to Accelerated Aging. Ind. Eng. Chem. 18, 420–424. https://doi.org/10.1021/ie50196a028

Jendrossek, D., 2019. Rubber oxygenases. Appl. Microbiol. Biotechnol. 103, 125–142. https://doi.org/10.1007/s00253-018-9453-z

Jendrossek, D., Reinhardt, S., 2003. Sequence analysis of a gene product synthesized by *Xanthomonas* sp. during growth on natural rubber latex. FEMS Microbiol. Lett. 224, 61–65. https://doi.org/10.1016/S0378-1097(03)00424-5

Jouan, X., Adam, C., Fromageot, D., Gardette, J.L., Lemaire, J., 1989. Microspectrophotometric determinations of product 'Profiles' in photooxidized matrices. Polym. Degrad. Stab. 25, 247–265. https://doi.org/10.1016/S0141-3910(89)81010-9

Karekar, A., Schicktanz, C., Tariq, M., Oßwald, K., Reincke, K., Cepus, V., Langer, B., Saalwächter, K., 2023. Effects of artificial weathering in NR/SBR elastomer blends. Polym. Degrad. Stab. 208, 110267. https://doi.org/10.1016/j.polymdegradstab.2023.110267

Kim, S., Kramer, R.W., Hatcher, P.G., 2003. Graphical Method for Analysis of Ultrahigh-Resolution Braodband mass spectra of Natural Organic Matter, the Van Krevelen diagram. Anal. Chem. 75, 5336–5344. https://doi.org/10.1021/ac034415p CCC:

Klöckner, P., Seiwert, B., Eisentraut, P., Braun, U., Reemtsma, T., Wagner, S., 2020. Characterization of tire and road wear particles from road runoff indicates highly dynamic particle properties. Water Res. 185, 116262. https://doi.org/10.1016/j.watres.2020.116262

Klöckner, P., Seiwert, B., Weyrauch, S., Escher, B.I., Reemtsma, T., Wagner, S., 2021.

Comprehensive characterization of tire and road wear particles in highway tunnel road dust by use of size and density fractionation. Chemosphere 279, 130530. https://doi.org/10.1016/j.chemosphere.2021.130530

Kourtchev, I., O'Connor, I.P., Giorio, C., Fuller, S.J., Kristensen, K., Maenhaut, W., Wenger, J.C., Sodeau, J.R., Glasius, M., Kalberer, M., 2014. Effects of anthropogenic emissions on the molecular composition of urban organic aerosols: An ultrahigh resolution mass spectrometry study. Atmos. Environ. 89, 525–532. https://doi.org/10.1016/j.atmosenv.2014.02.051

Koutny, M., Sancelme, M., Dabin, C., Pichon, N., Lemaire, J., Koutny, M., Sancelme, M., Dabin, C., Pichon, N., Delort, A.M., Lemaire, J., 2006. Acquired biodegradability of polyethylenes containing pro-oxidant additives. Polym. Degrad. Stab. 91, 1495–1503. https://doi.org/10.1016/j.polymdegradstab.2005.10.007

Lacoste, J., Adam, C., Siampiringue, N., Lemaire, J., 1994. Ozonation, a minor route for elastomer weathering. Eur. Polym. J. 30, 433–441. https://doi.org/10.1016/0014-3057(94)90040-X

Leads, R.R., Weinstein, J.E., 2019. Occurrence of tire wear particles and other microplastics within the tributaries of the Charleston Harbor Estuary, South Carolina, USA. Mar. Pollut. Bull. 145, 569–582. https://doi.org/10.1016/j.marpolbul.2019.06.061

Li, Y., Zhao, S., Wang, Y., 2012. Microbial Desulfurization of Ground Tire Rubber by *Sphingomonas* sp.: A Novel Technology for Crumb Rubber Composites. J. Polym. Environ. 20, 372–380. https://doi.org/10.1007/s10924-011-0386-1

Li, Y., Zhao, S., Zhang, L., Wang, Y., Yu, W., 2013. The effect of different Fe2+ concentrations in culture media on the recycling of ground tyre rubber by *Acidithiobacillus ferrooxidans* YT-1. Ann. Microbiol. 63, 315–321. https://doi.org/10.1007/s13213-012-0476-x

Linos, A., Berekaa, M.M., Reichelt, R., Keller, U., Schmitt, J., Flemming, H.C., Kroppenstedt, R.M., Steinbüchel, A., 2000. Biodegradation of cis-1,4-polyisoprene rubbers by distinct actinomycetes: Microbial strategies and detailed surface analysis. Appl. Environ. Microbiol. 66, 1639–1645.

https://doi.org/10.1128/AEM.66.4.1639-1645.2000

Linos, A., Steinbüchel, A., 1998. Microbial degradation of natural and synthetic rubbers by novel bacteria belonging to the genus Gordona. Kautschuk und Gummi Kunststoffe 51, 496–499.

Mertz, G., Hassouna, F., Leclère, P., Dahoun, A., Toniazzo, V., Ruch, D., 2012. Correlation between (nano)-mechanical and chemical changes occurring during photo-oxidation of filled vulcanised styrene butadiene rubber (SBR). Polym. Degrad. Stab. 97, 2195–2201. https://doi.org/10.1016/j.polymdegradstab.2012.08.008

Müller, K., Hübner, D., Huppertsberg, S., Knepper, T.P., Zahn, D., 2022. Probing the chemical complexity of tires: Identification of potential tire-borne water contaminants with high-resolution mass spectrometry. Sci. Total Environ. 802, 149799. https://doi.org/10.1016/j.scitotenv.2021.149799

Nguyen, L.H., Nguyen, H.D., Tran, P.T., Nghiem, T.T., Nguyen, T.T., Dao, V.L., Phan, T.N., To, A.K., Hatamoto, M., Yamaguchi, T., Kasai, D., Fukuda, M., 2020. Biodegradation of natural rubber and deproteinized natural rubber by enrichment bacterial consortia. Biodegradation 31, 303–317. https://doi.org/10.1007/s10532-020-09911-0

Nielsen, A.F., Polesel, F., Ahonen, T., Palmqvist, A., Baun, A., Hartmann, N.B., 2023. Assessing the Biodegradability of Tire Tread Particles and Influencing Factors. Environ. Toxicol. Chem. 43, 31–41. https://doi.org/10.1002/etc.5757

Noziere, B., Kalberer, M., Claeys, M., Allan, J., D'Anna, B., Decesari, S., Finessi, E., Glasius, M., Grgić, I., Hamilton, J.F., Hoffmann, T., Iinuma, Y., Jaoui, M., Kahnt, A., Kampf, C.J., Kourtchev, I., Maenhaut, W., Marsden, N., Saarikoski, S., Schnelle-Kreis, J., Surratt, J.D., Szidat, S., Szmigielski, R., Wisthaler, A., 2015. The Molecular Identification of Organic Compounds in the Atmosphere: State of the Art and Challenges. Chem. Rev. 115, 3919–3983. https://doi.org/10.1021/cr5003485

Odobel, C., Dussud, C., Philip, L., Derippe, G., Lauters, M., Eyheraguibel, B., Burgaud, G., Ter Halle,

A., Meistertzheim, A.L., Bruzaud, S., Barbe, V., Ghiglione, J.F., 2021. Bacterial Abundance, Diversity and Activity During Long-Term Colonization of Non-biodegradable and Biodegradable Plastics in Seawater. Front. Microbiol. 12, 734782. https://doi.org/10.3389/fmicb.2021.734782

Osswald, K., Reincke, K., Schossig, M., Sökmen, S., Langer, B., 2019. Influence of different types of antioxidants on the aging behavior of carbon-black filled NR and SBR vulcanizates. Polym. Test. 79, 106053. https://doi.org/10.1016/j.polymertesting.2019.106053

Panko, J.M., Chu, J., Kreider, M.L., Unice, K.M., 2013. Measurement of airborne concentrations of tire and road wear particles in urban and rural areas of France, Japan, and the United States. Atmos. Environ. 72, 192–199. https://doi.org/10.1016/j.atmosenv.2013.01.040

Parker-Jurd, F.N.F., Napper, I.E., Abbott, G.D., Hann, S., Thompson, R.C., 2021. Quantifying the release of tyre wear particles to the marine environment via multiple pathways. Mar. Pollut. Bull. 172, 112897. https://doi.org/10.1016/j.marpolbul.2021.112897

Potaufeux, J.E., Rapp, G., Barrau, S., Liu, G., Zhang, C., Giannelis, E.P., Notta-Cuvier, D., Lauro, F., Raquez, J.M., Odent, J., Therias, S., 2022. Influence of photooxidation on ionic reversible interactions of ionic poly(ether urethane)/silica hybrids. Polym. Degrad. Stab. 197, 109872. https://doi.org/10.1016/j.polymdegradstab.2022.109872

Rauert, C., Charlton, N., Okoffo, E.D., Stanton, R.S., Agua, A.R., Pirrung, M.C., Thomas, K. V., 2022. Concentrations of Tire Additive Chemicals and Tire Road Wear Particles in an Australian Urban Tributary. Environ. Sci. Technol. 56, 2421–2431. https://doi.org/10.1021/acs.est.1c07451

Rezig, N., Bellahcene, T., Aberkane, M., Nait Abdelaziz, M., 2020. Thermo-oxidative ageing of a SBR rubber: effects on mechanical and chemical properties. J. Polym. Res. 27, 339. https://doi.org/10.1007/s10965-020-02330-y

Rodrigo, O.-A., Daynet, S. del C., Jaime, N.-M., Nora, F., José, Á.-B., Alejandro, A., Jhonny, S.V., Milton, B.-A., 2021. Analysis of the degradation of polyethylene, polystyrene and polyurethane

mediated by three filamentous fungi isolated from the Antarctica. African J. Biotechnol. 20, 66–76. https://doi.org/10.5897/ajb2020.17200

Rose, K., Tenberge, K.B., Steinbüchel, A., 2005. Identification and characterization of genes from *Streptomyces* sp. strain K30 responsible for clear zone formation on natural rubber latex and poly(cis-1,4-isoprene) rubber degradation. Biomacromolecules 6, 180–188. https://doi.org/10.1021/bm0496110

Roy, R.V., Das, M., Banerjee, R., Bhowmick, A.K., 2006. Comparative studies on crosslinked and uncrosslinked natural rubber biodegradation by *Pseudomonas* sp. Bioresour. Technol. 97, 2485–2488. https://doi.org/10.1016/j.biortech.2005.09.024

Santo, M., Weitsman, R., Sivan, A., 2013. The role of the copper-binding enzyme - laccase - in the biodegradation of polyethylene by the actinomycete *Rhodococcus ruber*. Int. Biodeterior. Biodegrad. 84, 204–210. https://doi.org/10.1016/j.ibiod.2012.03.001

Seiwert, B., Nihemaiti, M., Troussier, M., Weyrauch, S., Reemtsma, T., 2022. Abiotic oxidative transformation of 6-PPD and 6-PPD quinone from tires and occurrence of their products in snow from urban roads and in municipal wastewater. Water Res. 212, 118122. https://doi.org/10.1016/j.watres.2022.118122

Seuront, L., Zardi, G.I., Uguen, M., Bouchet, V.M.P., Delaeter, C., Henry, S., Spilmont, N., Nicastro, K.R., 2022. A whale of a plastic tale: A plea for interdisciplinary studies to tackle micro- and nanoplastic pollution in the marine realm. Sci. Total Environ. 846, 157187. https://doi.org/10.1016/j.scitotenv.2022.157187

Sharma, V., Siedenburg, G., Birke, J., Mobeen, F., Jendrossek, D., Prakash, T., 2018. Metabolic and taxonomic insights into the Gram-negative natural rubber degrading bacterium *Steroidobacter cummioxidans* sp. nov., strain 35Y. PLoS One 13, 1–20. https://doi.org/10.1371/journal.pone.0200399

Sinturel, C., Billingham, N.C., 2000. A theoretical model for diffusion-limited oxidation applied to

oxidation profiles monitored by chemiluminescence in hydroxyterminated polybutadiene. Polym. Int. 49, 937–942. https://doi.org/10.1002/1097-0126(200009)49:9<937::AID-PI399>3.0.CO;2-8

Sueur, M., Maillard, J.F., Lacroix-Andrivet, O., Rüger, C.P., Giusti, P., Lavanant, H., Afonso, C., 2023. PyC2MC: An Open-Source Software Solution for Visualization and Treatment of High-Resolution Mass Spectrometry Data. J. Am. Soc. Mass Spectrom. 34, 617–626. https://doi.org/10.1021/jasms.2c00323

Thomas, J., Moosavian, S.K., Cutright, T., Pugh, C., Soucek, M.D., 2022. Investigation of abiotic degradation of tire cryogrinds. Polym. Degrad. Stab. 195, 109814. https://doi.org/10.1016/j.polymdegradstab.2021.109814

Tsuchii, A., Suzuki, T., Fukuoka, S., 1984. Bacterial Degradation of 1,4-Type Polybutadiene. Agric. Biol. Chem. 48, 621–625. https://doi.org/10.1271/bbb1961.48.621

Tsuchii, A., Suzuki, T., Takahara, Y., 1979. Microbial degradation of cis-1, 4-polyisoprene. Agric. Biol. Chem. 43, 2441–2446. https://doi.org/10.1080/00021369.1979.10863857

Tsuchii, A., Suzuki, T., Takeda, K., 1985. Microbial degradation of natural rubber vulcanizates. Appl. Environ. Microbiol. 50, 965–970. https://doi.org/10.1128/aem.50.4.965-970.1985

Tsuchii, A., Takeda, K., Tokiwa, Y., 1996. Degradation of the rubber in truck tires by a strain of Nocardia. Biodegradation 7, 405–413. https://doi.org/10.1007/bf00056424

Tsuchii, A., Tokiwa, Y., 1999. Colonization and disintegration of tire rubber by a colonial mutant of Nocardia. J. Biosci. Bioeng. 87, 542–544. https://doi.org/10.1016/S1389-1723(99)80108-X

Unice, K.M., Bare, J.L., Kreider, M.L., Panko, J.M., 2015. Experimental methodology for assessing the environmental fate of organic chemicals in polymer matrices using column leaching studies and OECD 308 water/sediment systems: Application to tire and road wear particles. Sci. Total Environ. 533, 476–487. https://doi.org/10.1016/j.scitotenv.2015.06.053

Unice, K.M., Kreider, M.L., Panko, J.M., 2012. Use of a deuterated internal standard with pyrolysis-GC/MS dimeric marker analysis to quantify tire tread particles in the environment. Int. J.

975 Environ. Res. Public Health 9, 4033–4055. https://doi.org/10.3390/ijerph9114033

976 Van Krevelen, D.W., 1950. Graphical- statistical method for the study of structure and reaction
977 processes of coal. Fuel 29, 269–284.

978 Wagner, S., Klöckner, P., Reemtsma, T., 2022. Aging of tire and road wear particles in terrestrial and
979 freshwater environments – A review on processes, testing, analysis and impact. Chemosphere
980 288, 132467. https://doi.org/10.1016/j.chemosphere.2021.132467

981 Warneke, S., Arenskötter, M., Tenberge, K.B., Steinbüchel, A., 2007. Bacterial degradation of
982 poly(trans-1,4-isoprene (gutta percha). Microbiology 153, 347–356.
983 https://doi.org/10.1099/mic.0.2006/000109-0

984 Wilhelm, C., Gardette, J., 1994. Infrared identification of carboxylic acids formed in polymer
985 photooxidation. J. Appl. Polym. Sci. 51, 1411–1420.
986 https://doi.org/10.1002/app.1994.070510808

987 Williams, G.R., 1982. The Breakdown Of Rubber Polymers By Microorganisms. Int. Biodeterior.
988 Bull. 18, 31–36.

989